DTIC FILE COPY

(1)

AD-A202 662

ELECTRO-ENCEPHALOGRAM BASED ADAPTIVE ESTIMATION OF MAGNETO-ENCEPHALOGRAM SIGNALS

THESIS

Roger A. Wood
Captain, USAF

AFIT/GE/ENG/88D-62

DTIC
ELECTE
JAN 17 1989
S
D

DISTRIBUTION STATEMENT A
Approved for public release
Distribution Unlimited

DEPARTMENT OF THE AIR FORCE
AIR UNIVERSITY
AIR FORCE INSTITUTE OF TECHNOLOGY
Wright-Patterson Air Force Base, Ohio

89 1 17 125

(1)

AFIT/GE/ENG/88D-62

ELECTRO-ENCEPHALOGRAM BASED ADAPTIVE ESTIMATION OF MAGNETO-ENCEPHALOGRAM SIGNALS

THESIS

Roger A. Wood
Captain, USAF

AFIT/GE/ENG/88D-62

DTIC
ELECTE
JAN 17 1989
S D
CD

Approved for public release; distribution unlimited

AFIT/GE/ENG/88D-62

ELECTRO-ENCEPHALOGRAM BASED ADAPTIVE ESTIMATION OF MAGNETO-ENCEPHALOGRAM SIGNALS

THESIS

Presented to the Faculty of the School of Engineering
of the Air Force Institute of Technology
Air University
In Partial Fulfillment of the
Requirements for the Degree of
Master of Science in Electrical Engineering

Roger A. Wood, B.S.
Captain, USAF

December 1988

Accesion For
NTIS
DTIC
Unannounced
Justification
By
Distribution
Availability Codes
Dist
A-1

Approved for public release; distribution unlimited

Preface

The purpose of this study was to filter unwanted background noise from the evoked response field of the magneto-encephalogram using adaptive processing techniques. An adaptive filter, using the evoked response potential signal obtained from electro-encephalogram measurements, was used to enhance the evoked response field signal. Accurate signal estimation of evoked response fields is a necessary requirement for future brain studies involving visual and audio stimulus responses.

No special knowledge or background is required to understand this research, although some knowledge of digital signal processing may be helpful in understanding the concepts of adaptive filtering. A general discussion of adaptive filter theory is included in Chapter Two.

Several individuals greatly influenced the direction of this research. I would like to thank my advisor, Capt Rob Williams, who conceptualized this study and helped to develop its overall scope and goals along with the other committee members who offered their support and advice. A special thanks is owed to Capt Paul DeRego and the rest of the people at the magnetoencephalography lab at AAMRL who never complained despite my late friday afternoon data collection runs. Finally, I owe my wife [redacted] and daughters [redacted] a very special thanks for the support that only a family can provide.

Roger A. Wood

Table of Contents

List of Figures

Abstract

Adaptive signal processing techniques were used to filter out unwanted background noise from the evoked response field signals obtained from magneto-encephalogram measurements. A model of the evoked response field signals was first developed to test the adaptive algorithm in an environment corrupted by white gaussian noise. Several modeling experiments verified the feasibility of adaptive filtering using an enhancement design with a correlated signal representing the evoked potential response obtained from electro-enchephalogram measurements. The experimental results showed that signal estimation is improved by a strong correlation between the evoked response field and evoked response potential.

Following the modeling experiments, filtering of actual evoked responses was attempted. To obtain the evoked field data, an audio or visual stimulus was provided to a test subject located inside a shielded chamber. Time sequenced electro-encephalogram and magneto-encephalogram signals were recorded for later processing using an adaptive filter based on the least-mean-square algorithm. Accuracy of the filtered human data could not be quantified due to a lack of a priori knowledge of the exact signals before filtering. Comparisons of filtered responses with ensemble averaged responses of up to 80 signals showed waveform similarities.

ELECTRO-ENCEPHALOGRAM BASED ADAPTIVE ESTIMATION OF MAGNETO-ENCEPHALOGRAM SIGNALS

I. Introduction

Background

The Air Force Armstrong Aerospace Medical Research Laboratory (AAMRL), Human Engineering Division, is currently studying localization of brain activity and its relationship to physical stimuli. The analysis of magneto-encephalogram (MEG) signals is an important part of this research due to its non-invasive method of detection. One of AAMRL's research goals is the detection and estimation of single evoked neural responses. Of particular interest is the localization of brain activity in response to a visual or audio stimulus. An improvement in the measurement accuracy of these responses by filtering noise components of the MEG could significantly improve localization.

Problem

The purpose of this research is to investigate the application of adaptive signal processing techniques, based on the statistical relationship between MEG and electro-encephalogram (EEG) signals, to enhance the MEG using an EEG reference.

Summary of Current Knowledge

Current research has shown that electromagnetic field measurements of the brain can be used as a non-invasive method of localizing brain activity (7:222). Two measurement and recording techniques, the MEG and the EEG, detect the weak magnetic and electric fields associated with the electro-chemical operation of the brain. The MEG and the EEG evoked responses are difficult to accurately detect due to their relatively small measurement amplitudes compared to various sources of noise. Noise filtering of the MEG is of the most interest because evoked magnetic field measurements hold greater promise than evoked potential signals in accurately localizing brain activity.

An adaptive system is time-varying and self-adjusting. Whereas a fixed (linear) system is designed to operate under a strict set of input conditions and performance criteria, the adaptive system continually seeks an optimum performance based on input conditions that may not be fully known (11:4). The time-varying nature of MEG signals lead to the possibility of applying adaptive filtering to the problem of removing noise related to physiological sources. A signal enhancing adaptive filter can be applied to MEG signals using the EEG as a reference signal. This method of filtering can be applied if there is correlation between the two signals. The relationship of electric currents and magnetic fields and observed similarities of signal charac-

teristics suggest a correlation; however, the question of correlation has not been definitively answered (1:473-475).

Assumptions

A statistical analysis of MEG and EEG signals will be undertaken in this research. The raw data for this analysis was obtained from AAMRL and is assumed to be accurate. No analysis of data errors is included in this research. This assumption is required due to the difficulty in defining the accuracy of the recorded data.

Scope

This study includes a statistical analysis of MEG and EEG signals and the development of an adaptive filter computer model to process simulated MEG and EEG signals. Processing of actual MEG and EEG signals with a computer implemented adaptive filter is attempted based on the knowledge gained from the simulated implementation.

Approach/Methodology

The following steps were followed in solving this problem:

(1) Analyze the signal and noise characteristics of the MEG and EEG measurement system.

(2) Perform a statistical study of MEG and EEG signals using digital signal processing techniques and use the results of this study to develop models of evoked response field and evoked response potential signals.

(3) Develop an adaptive filter using the EEG signal model with noise to enhance the MEG signal model with noise and compare the results to the signal models before noise was added.

(4) Analyze the performance of the adaptive filter using real human MEG and EEG signals and make recommendations.

Materials and Equipment

The MEG and EEG data was obtained from AAMRL. This data was recorded on a floppy disk for processing on a personal computer. The statistical analysis of these signals was accomplished using a software package called DADiSP by DSP Development Corporation. The adaptive filter and simulated MEG and EEG signals were implemented on a personal computer. A more detailed description of the data collecting equipment is available in Chapter IV.

II. BACKGROUND

Introduction

It has been shown that electromagnetic field measurements can be used to localize brain activity sources related to a specific stimulus (7:222). Two measurement and recording techniques, the electro-encephalogram (EEG) and the magneto-encephalogram (MEG), detect the weak electric and magnetic fields associated with the electro-chemical operation of the brain.

To simplify notation throughout this thesis, the MEG evoked field will be referred to as an evoked response field or simply ERF. The EEG evoked potential will be called an evoked response potential or ERP. Further, background MEG signals or field measurements not associated with a specific stimulus, will be referred to as the MEG. Likewise, background EEG signals, electrical potentials not related to the stimulus, will be called the EEG.

The ERP and ERF signals are difficult to accurately detect due to their relatively small measurement amplitudes compared to various sources of noise and distortion. This is particularly true of the ERF (6:842). This review will focus on current knowledge of the ERF and present a method of filtering the background MEG to improve brain activity localization.

Noise filtering of ERF signals using adaptive signal processing methods will be investigated. Adaptive systems

can automatically self-optimize in relation to a constantly changing environment and therefore have application in several fields of signal processing; however, this review will focus on noise canceling and signal enhancing adaptive filters. (11:4)

A detailed discussion of ERF characteristics will be followed by a review of adaptive signal processing. Finally, methods of filtering MEG signals using adaptive filtering techniques will be presented.

The Magneto-Encephalogram

Brain activity is characterized by electrical pulses produced in response to some stimulus. This electro-chemical process occurs specifically in the neuron or nerve cell. Communication between neurons is accomplished through a complex network which provides many inputs to the neuron but only one output. A current pulse is produced at the output of a neuron only when the summation of input currents exceeds a particular threshold. Propagation of current pulses through this network of neurons is the basis of all brain computation and communication. (4:3)

Electro-encephalogram measurements are obtained by measuring surface potentials caused by induced cellular currents related to brain activity. The first measurement of this kind was by Burger in 1929 (1:469). The general state of the brain can be interpreted by the evaluation of the EEG wave frequency, amplitude, form, periodicity, and

the locations of the measurement electrodes. Frequencies of interest are generally low (from 0.5 to 15 hertz) and amplitudes are measured in microvolts. The analysis of normal and abnormal EEG patterns using the above criteria are used as a basis for determining neural abnormalities. (4:9)

Magneto-encephalography is a non-invasive method of analyzing brain activity by measuring and recording magnetic fields above the surface of the head (4:10). The signal characteristics of the MEG are similar to the EEG because they are produced by the same electro-chemical neural currents. However, the MEG has a greater susceptibility to noise than the EEG due to its much smaller amplitude. For this reason, the MEG was not accurately measured until 43 years after the first EEG measurements when a highly accurate device to detect the weak magnetic fields was introduced. Cohen's first direct MEG trace was recorded in 1967. Since then, magnetic fields suggesting sharp localization of brain activity have been discovered. (2:9)

Detection of the brain's magnetic fields is accomplished by using a Superconducting Quantum Interference Device (SQUID). The SQUID takes advantage of the measureable response of a superconducting current loop due to the presence of a magnetic flux density (4:17). An important advantage of the MEG over the EEG is that the SQUID can detect field components from sources close to the sensor

(3:11). The SQUID is designed to be sensitive enough to detect the weak magnetic fields produced by brain activity while also eliminating background noise caused by room lights or machinery (6:842). However, distortion of MEG signals is also caused by sources that cannot be eliminated by conventional analog or digital filtering techniques. This noise is related to physiological sources such as head and body movements, muscle activity and eye movement (6:842).

Adaptive Signal Processing

An adaptive system is time-varying and self-adjusting. Whereas a fixed (linear) system is designed to operate under a strict set of input conditions and performance criteria, the adaptive system continually seeks an optimum performance based on input conditions that may not be fully known (11:5). Adaptive systems are usually nonlinear and are therefore difficult to analyze. This disadvantage is outweighed by the increased system performance obtained under unknown input conditions (11:4).

Most applications of adaptive processing use a closed loop design. A generalized block diagram of a closed loop adaptive filter is shown in figure 2.1. The output of the processor is compared with some known model of the desired signal. The difference between these two signals is called the error signal. The adaptive algorithm adjusts the

overall response of the system by minimizing the error. This is accomplished by continuously adjusting the operating paremeters of the system processor. (11:20-21)

Adaptive filtering is typically implemented as a finite impulse response filter or adaptive linear combiner with varying weights as represented in figure 2.2. The output of a combiner having k discrete inputs can be written as

$$y(k) = \sum_{n=0}^{N} w_n(k)x(k-n) \qquad (2.1)$$

where

$x(k-n)$ = value of $(k-n)$th input
$y(k)$ = kth output of combiner
$w_n(k)$ = value of weight n for input k.

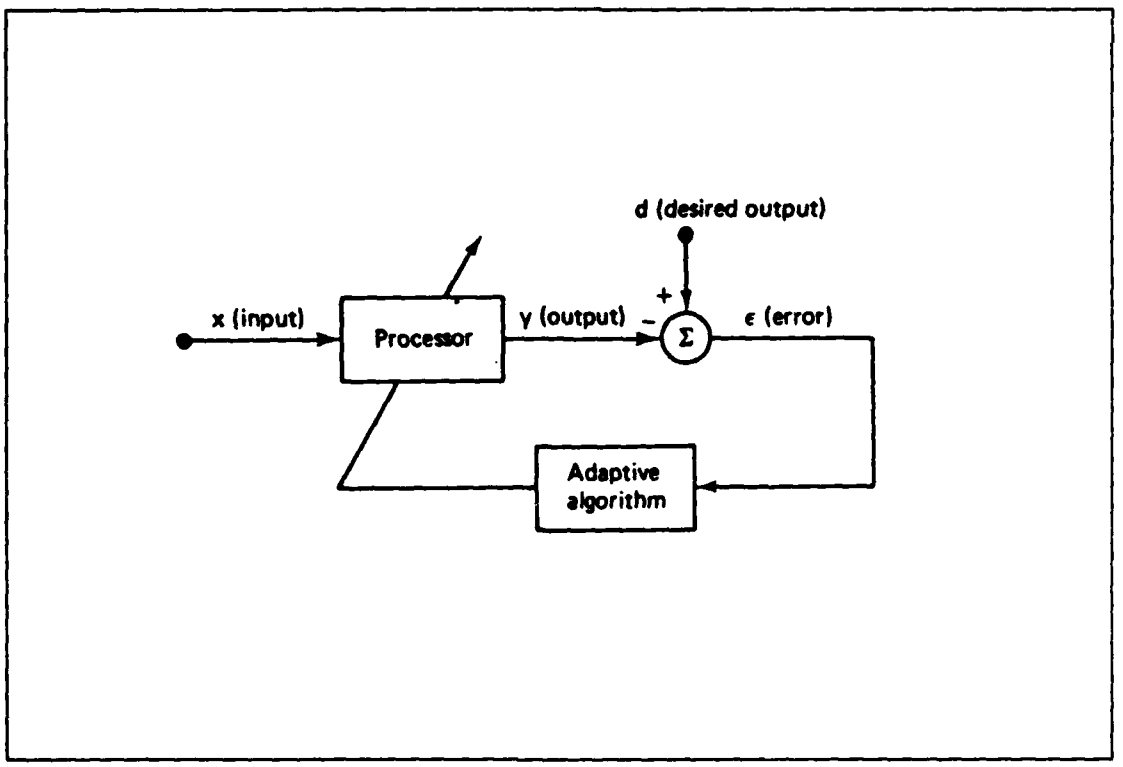

Figure 2.1. Generalized Adaptive Filter (11:9)

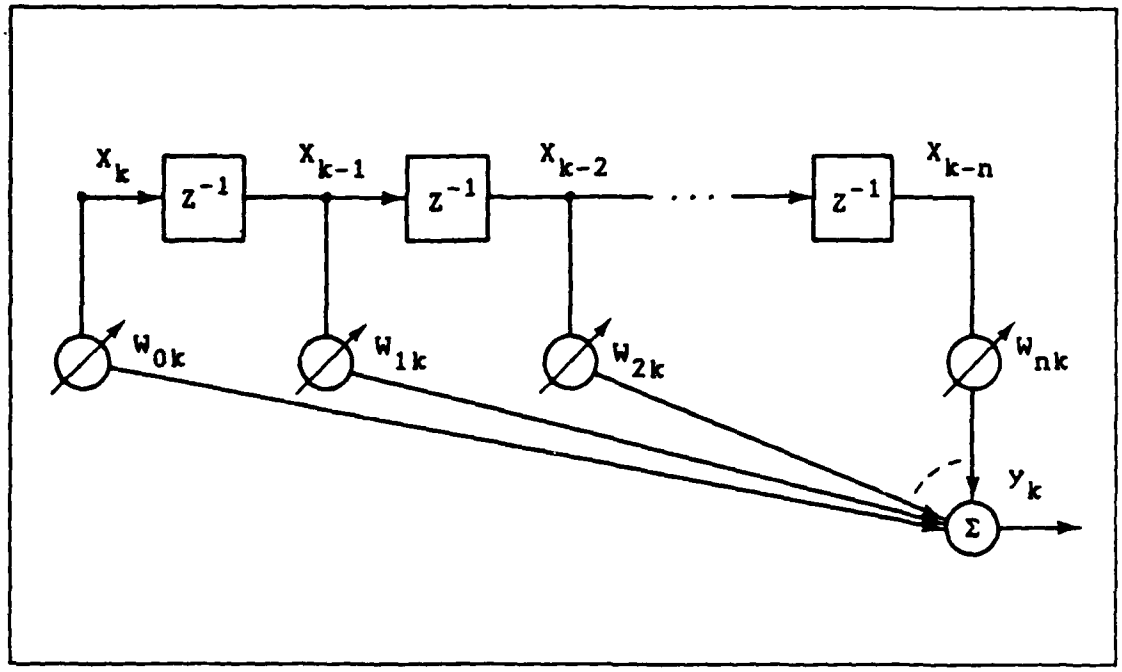

Figure 2.2. Adaptive Linear Combiner (11:17)

Defining the weight vector of the combiner as

$$\underline{W}(k) = [w_0(k) \quad w_1(k) \quad w_2(k) \cdots \quad w_n(k)]^T, \tag{2.2}$$

equation 2.1 can be rewritten as

$$y(k) = \underline{W}(k)^T\underline{X}(k) \tag{2.3}$$

where $\underline{X}(k)$ is the input vector. The weight vector depends on the output and the desired response. The adaptive process minimizes the average power of the error signal or mean-square value defined by the following equations:

$$\varepsilon(k) = d(k) - y(k) \tag{2.4}$$

$$= d(k) - \underline{W}(k)\underline{X}(k) \tag{2.5}$$

$$\varepsilon(k)^2 = [d(k) - \underline{W}(k)^T\underline{X}(k)]^2 \tag{2.6}$$

$$\varepsilon(k)^2 = d(k)^2 - 2 \cdot d(k)\underline{X}(k)^T\underline{W}(k) + \underline{X}(k)^T\underline{W}(k)\underline{W}(k)^T\underline{X}(k). \tag{2.7}$$

Then by taking the expected value of the square of the error and assuming that $\underline{X}$ and $\underline{W}$ are uncorrelated, the mean-square-error is defined as:

$$MSE = E[\varepsilon(k)^2] = E[d(k)^2] + E[\underline{W}^T\underline{X}(k)\underline{X}(k)^T] - E[2 \cdot d(k)\underline{X}(k)^T\underline{W}] \quad (2.8)$$

$$= E[d(k)]^2 + \underline{W}^T E[\underline{X}(k)\underline{X}(k)^T]\underline{W} - 2 \cdot E[d(k)\underline{X}(k)^T]\underline{W} \quad (2.9)$$

$$= E[d(k)]^2 + \underline{W}^T\underline{R}\underline{W} - 2 \cdot \underline{P}^T\underline{W} \quad (2.10)$$

where $\underline{R}$ is the input correlation matrix and $\underline{P}$ is the cross-correlation matrix between the desired signal and the input signal. (11:15-26)

When the input signal and desired signal are statistically stationary, the MSE is a quadratic function of the filter weight components. This quadratic function forms a performance surface on which the adaptive algorithm will continuously seek a minimum value. An example of a two weight performance surface is shown in figure 2.3. Most adaptive processes find the minimum of the performance surface by gradient methods. The following definition for the gradient is used:

$$\nabla = \frac{\delta(MSE)}{\delta\underline{W}} = \left[\delta(MSE) \quad \delta(MSE) \cdots \delta(MSE) \right]^T \quad (2.11)$$

$$= 2 \cdot \underline{R}\underline{W} - 2\underline{P}. \quad (2.12)$$

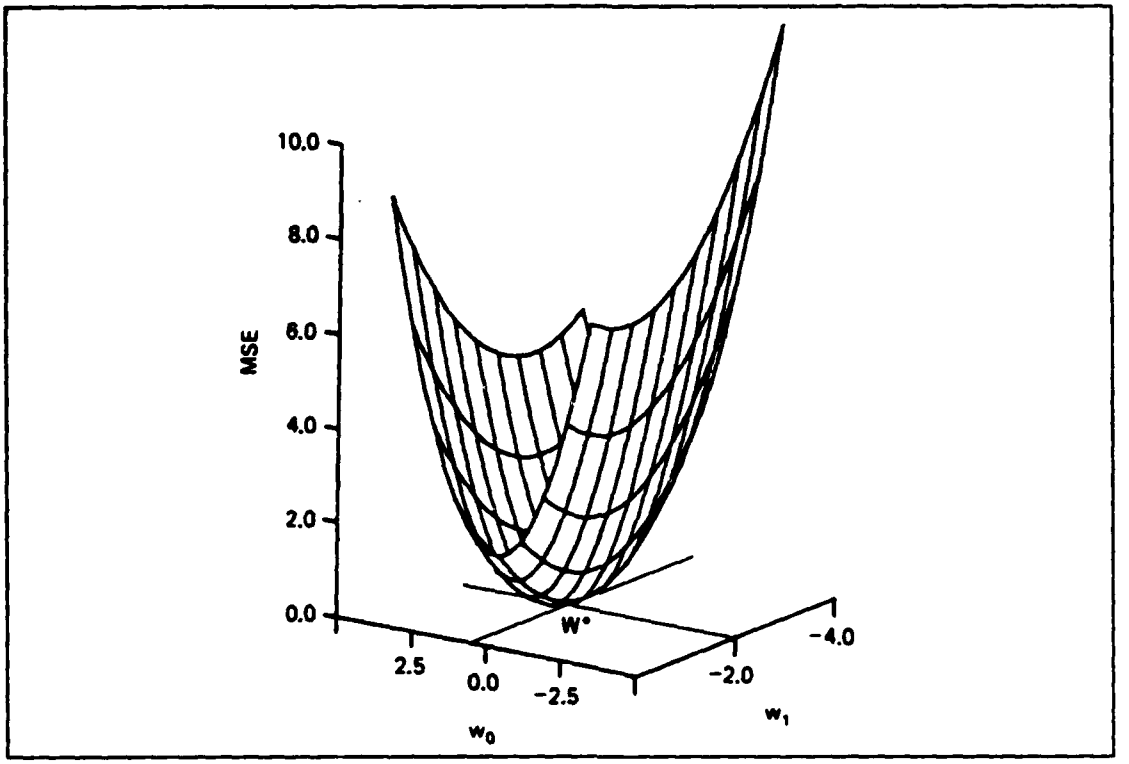

Figure 2.3. A Two Weight Performance Surface (11:25)

The minimum mean-square-error (MMSE) is obtained by setting equation 2.12 equal to zero:

$$2 \cdot \underline{R}\underline{W}^* - 2\underline{P} = 0 \tag{2.13}$$

where $\underline{W}^*$ is defined as the optimum weight vector. As long as there exists an inverse for $\underline{R}$, the optimum weight vector can then be defined as

$$\underline{W}^* = R^{-1}P. \tag{2.14}$$

Finally, by substituting equation 2.13 into equation 2.9 the minimum MSE is obtained:

$$\text{MMSE} = E[d(k)^2] + \underline{W}^{*T}\underline{R}\underline{W}^* - 2\underline{P}^T\underline{W}^* \tag{2.15}$$

and after simplifying,

$$\text{MMSE} = E[d(k)^2] - \underline{P}^T\underline{W}^*. \tag{2.16}$$

The minimum MSE is represented in figure 2.3 as the bottom point on the parabolic surface. (11:15-27)

A typical adaptive algorithm adjusts the system parameters by determining the gradient of the mean-square error of the system inputs (11:20). The gradient is set equal to zero to obtain a minimum mean-square error of the adaptive process (11:21). Two algorithms used to determine this minimum are Newton's method and the steepest descent method (11:99). Each iteration of these algorithms requires an estimate of the gradient of the mean-square error (11:99).

A simpler and more commonly used algorithm is implemented by approximating the steepest descent method. This is called the least-mean-square (LMS) algorithm (11:100, 9:67). Its implementation is typically restricted to non-recursive adaptive filtering techniques which are of primary interest in this research. Instead of taking the gradient estimations of the mean-square error at each iteration, the LMS algorithm simply estimates the gradient by replacing the mean-square error with the square of the error. This deletes the complex requirement of estimating the gradient by averaging the square of the error. Using the steepest descent method, the filter weights were iteratively updated requiring that the gradient of the mean-square error be calculated during every iteration:

$$\underline{W}(k+1) = \underline{W}(k) - \mu\nabla(k) \qquad (2.17)$$

where μ is a convergence factor used to insure stability of the filter as well as control the speed of operation and noise. Since the LMS algorithm estimates the gradient by using the square of the error, the weight update equation becomes

$$\underline{W}(k+1) = \underline{W}(k) + 2\mu e(k)\underline{X}(k) \qquad (2.18)$$

where the convergence factor is 2μ. Without the averaging process used in the steepest descent method, a noise component is retained. However, the adaptive process acts as a low-pass filter to attenuate this noise. (11:99-103)

Adaptive Filtering of MEG Signals

A useful method of EEG and MEG signal estimation is to average many short periods of measurement related to an actual stimulus. Additional improvement of these event related signal estimates has been obtained by applying Weiner or minimum mean-square error (MMSE) filtering. Results of this technique have been mixed because MMSE filtering requires a stationary signal. The actual characteristics of ERP and ERF signals must be known to accurately apply MMSE filtering. (6:835)

The time-varying nature of ERF and ERP signals lead to the possibility of applying adaptive filtering to the problem of removing noise related to physiological sources. An interference canceler (shown in figure 2.4) can filter the noise component of the signal. The interference

canceler produces a signal at the output of the adaptive processor (y) that is very similar to the noise component of the signal plus noise. After a subtraction process, the output of the system closely resembles the original signal without noise (11:11). The noise component of the signal plus noise and the noise input to the adaptive processor (x) must be different signals that exhibit the properties of statistical correlation to one another.

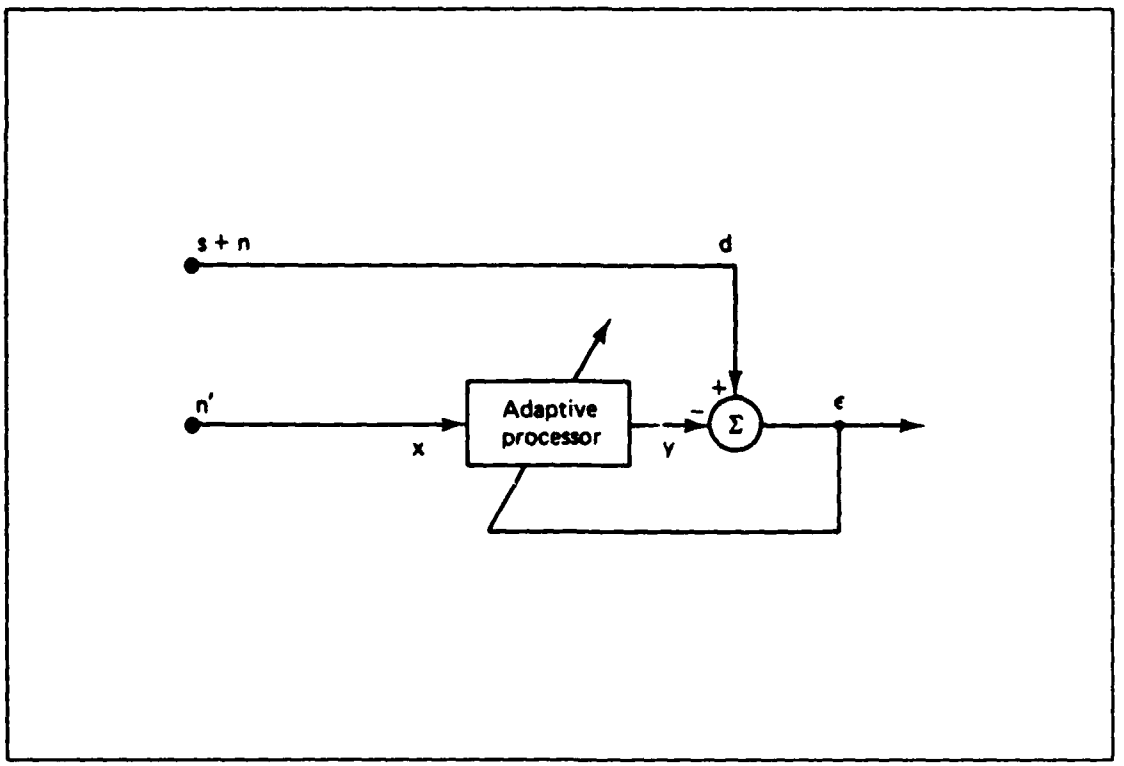

Figure 2.4. Interference Canceler (11:10)

There are several successful examples of adaptive noise canceler implementations. Thakor has shown that a noise canceling adaptive filter can reduce the number of ensemble averages required to accurately measure evoked potentials (9:6). A noise canceling adaptive filter was applied by Yama et al. to remove unwanted eye-blink noise from EEG signals (15:860).

Uncertainty of the statistical characteristics of the ERF and ERP signals make the interference canceler of figure 2.4 a less than desirable method of filtering MEG noise. There is no documented evidence of correlation between the ERP and ERF. Without correlation, there is no basis for proper noise cancelation. However, the block diagram in figure 2.4 can be modified slightly to implement a signal enhancer instead of a noise canceler. The only change needed is to use the output of the adaptive processor as the output of the system (14). Detection of the mimumum error by the adaptive processor means that the output of the adaptive processor (y) and the signal plus noise input (d) are nearly matched. Thus, the output of the system is an enhanced version of the signal plus noise input.

The above signal enhancing adaptive filter scheme can be applied to ERF and ERP signals if there is correlation between the two signals. The relationship of electric currents and magnetic fields along with observed similarities of signal characteristics suggest a correlation;

however, the question of correlation has not been definitively answered (1:473-475).

Since the ERF signal holds more promise in locating sources of brain activity, application of the signal enhancing adaptive filter would emphasize the ERF by designating it as the desired signal. In reference to the above discussion of the signal enhancer, the ERF signal would replace the signal plus noise input (d) to the filter and the input to the processor (x) would be the ERP signal.

III. Experimental Procedure

This chapter will describe the experimental configuration and procedures used in recording ERF and ERP data. The methods used in generating the stimulus will be presented first, followed by a discussion of the Superconducting Biomagnetometer, and finally a review of how the data was recorded.

Figure 3.1 is a block diagram of the experimental apparatus showing the stimulus generator, the superconducting biomagnetometer, and data gathering equipment. All experimental equipment is located in the Biomagnetic Laboratory at the Armstrong Aerospace Medical Research Labaratory (AAMRL).

Stimulus Generation

The experimental configuration was set up to provide either a visual stimulus or an audio stimulus. The configuration of the visual stimulus is shown in figure 3.2 and the audio test configuration is shown in figure 3.3. The visual stimulus was a flash of light projected through a translucent checkerboard screen. The duration of the flash was controlled by a waveform generator that triggered a servo controlled shutter mounted to the light source. This trigger was also supplied to the Masscomp 5400 computer as a time reference. The duration of the visual stimulus was 0.02 seconds with a 0.1 second pre-trigger interval. The

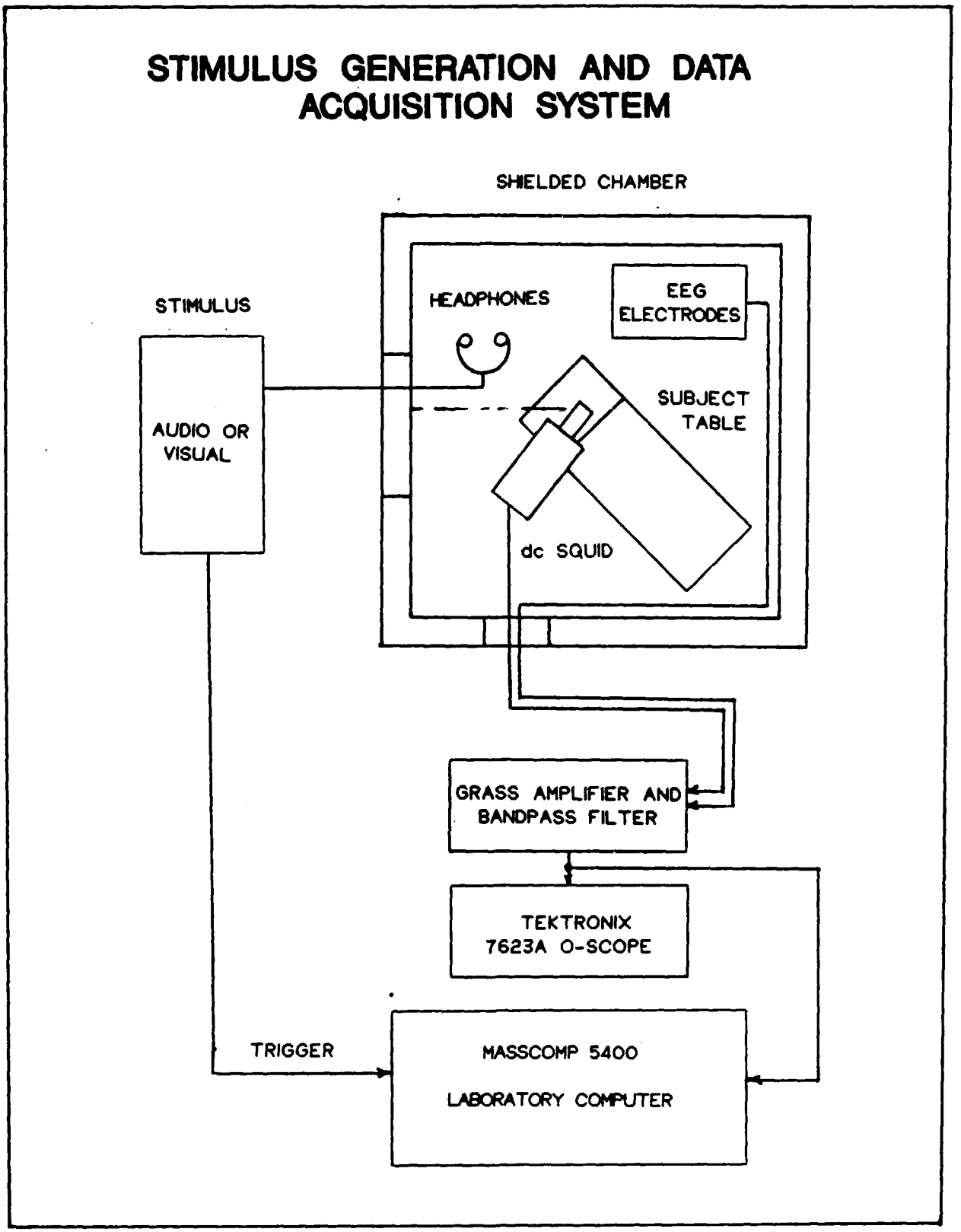

Figure 3.1. Experimental Configuration

total time duration of each experimental trial was 0.5 seconds. A red light-emitting-diode was mounted on the checkerboard screen to provide a point of focus for the test subject. The subject viewed the checkerboard screen through the chamber entrance. Placement of the measurement equipment required that the subject lay face down on the table and view the screen through a mirror that was aligned to provide a full view of the screen. The subject's face was supported by foam padding to provide stability and comfort. Holes were cut in the padding for breathing and visual access to the stimulus.

The audio stimulus was provided by three separate function generators. The resultant waveform from the output of the third function generator was a modulated pulse with a 600 hertz carrier and a total duration of 0.08 seconds. The first function generator also supplied a timing trigger to the Masscomp 5400 computer. The modulated signal was amplified and converted to an audio tone supplied by a horn driver. Vinyl tubing carried the audio tone into the shielded chamber. The tubing was fed into two plastic ear plugs worn by the test subject. A single test trial, with a total duration of 0.5 seconds, consisted of a 0.1 second pre-trigger or waiting period, the 0.08 second tone and a response period of 0.32 seconds.

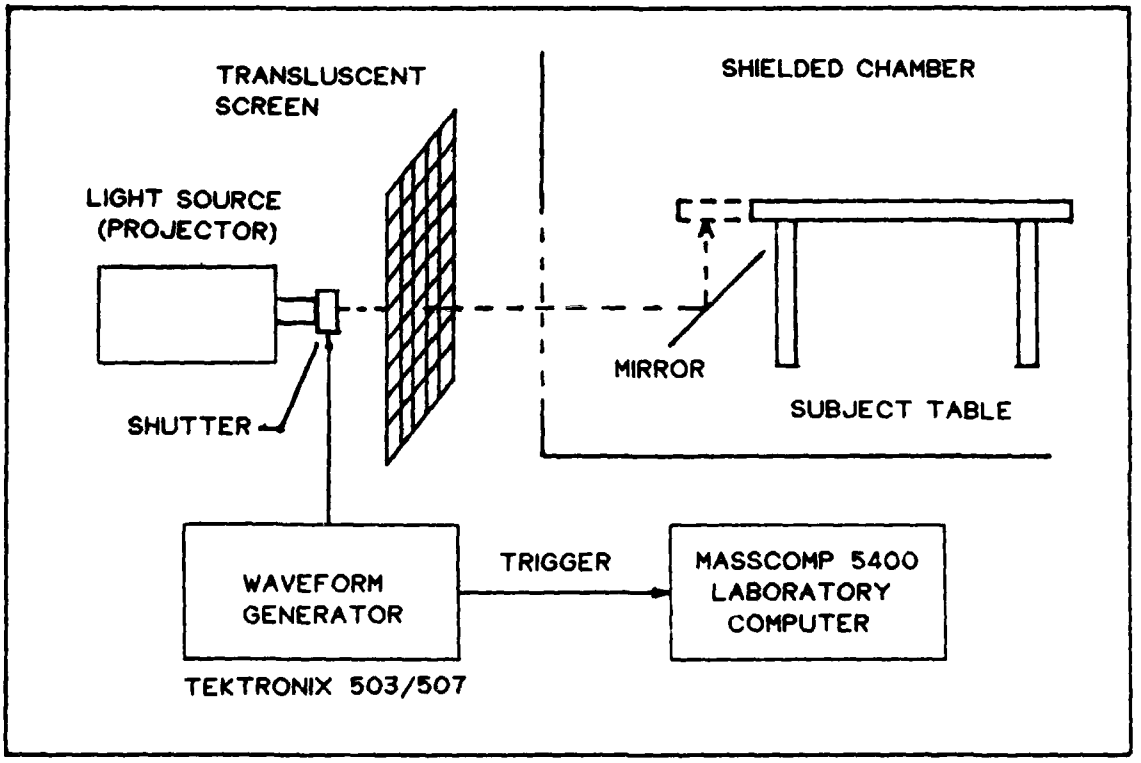

Figure 3.2. Visual Stimulus

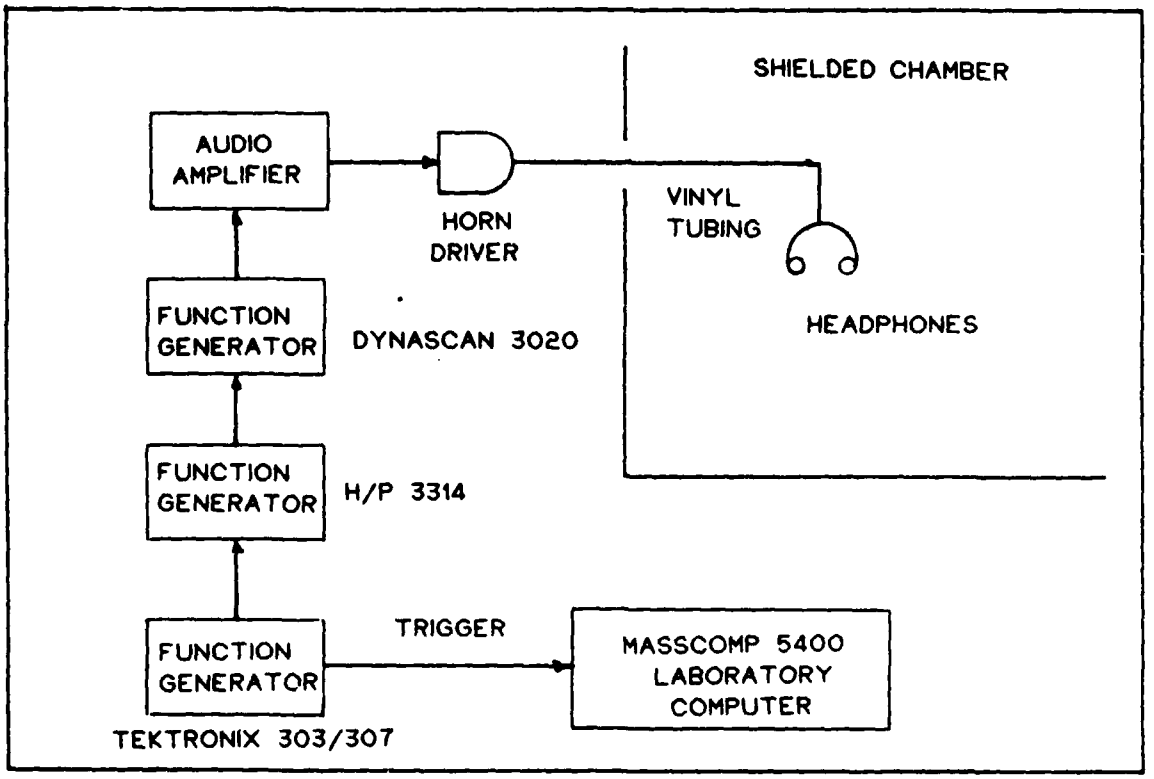

Figure 3.3. Audio Stimulus

Superconductive Biomagnetometer

As shown in figure 3.1, the biomagnetometer consists of a dc superconducting quantum interference device (SQUID) located within a shielded chamber. The SQUID measures the biomagnetic waves associated with brain activity or as defined previously, the magneto-encecephalogram (MEG). In addition to the MEG, electrical potential waveforms or electro-encephalograms (EEG) are also recorded within the chamber via electrodes mounted to the test subject's scalp. Both MEG and EEG data are collected within the shielded chamber as a visual or audio stimulus is provided to a test subject. As discussed previously, the waveforms measured as a direct result of a stimulus are called the ERF for evoked response field and ERP for evoked response potential.

The shielded chamber is designed to restrict electromagnetic waves from entering the test area and adversely affecting the data. The dc SQUID is particularly sensitive to electromagnetic interference. The chamber is enlosed on all sides and the data is collected close to the chamber's center to maximize the shielding effect. The walls of the shielded chamber are constructed of two layers of permalloy having a very high relative permeability. External fields are attenuated by the enclosure because the lines of magnetic flux are concentrated around the exterior walls due to their high relative permeability. (5:59)

Magnetic flux changes associated with brain activity

are detected by the dc SQUID. This thesis will not go into a detailed account of SQUID theory; however, several references, including DeRego and Dowler, are available. The SQUID is actually constructed using several superconducting loops as detectors. This particular configuration is called a second order gradiometer. The gradiometer loops are made of niobium metal: a superconductor at 9.2°Kelvin. All superconducting components of the squid are held at a constant temperature of 4.2°Kelvin by submerging them in a dewar of liquid helium. The dewar and detection components are housed in super insulated fiberglass mounted on a gimbel which can be positioned above the test subject's head. The gradiometer components are located in a thin tube that protrudes from the bottom of the dewar. This tube is placed directly against the subject's head when MEG measurements are being recorded. (5:51-60, 4:42-44)

A thin elastic cap with one centimeter spaced grid lines was placed over the subject's scalp as a measurement location reference. The zero-zero point of the grid is located at the inion (a protrusion of bone at the back of the skull). For both visual and audio measurements, the SQUID was placed typically at three centimeters left of a line separating the head from the bridge of the nose (the nasion) to the inion and seven centimeters up from the inion (see figure 3.4). Placement of the EEG electrodes depended on the type of response. For visual responses, electrodes

were placed in the O1 position which is defined as 10% up from the inion and 10% down from the Cz point. This is more clearly shown in figure 3.4. For audio responses, the electrodes were located at the C3 or C4 position; 50% up from the bridge of the nose and 10% down from Cz (see figure 3.4). In addition to the measurement electrodes, reference electrode were mounted behind the subject's ears and ground electrodes were located on the chin. All electrodes were applied directly to the scalp or skin with an adhesive.

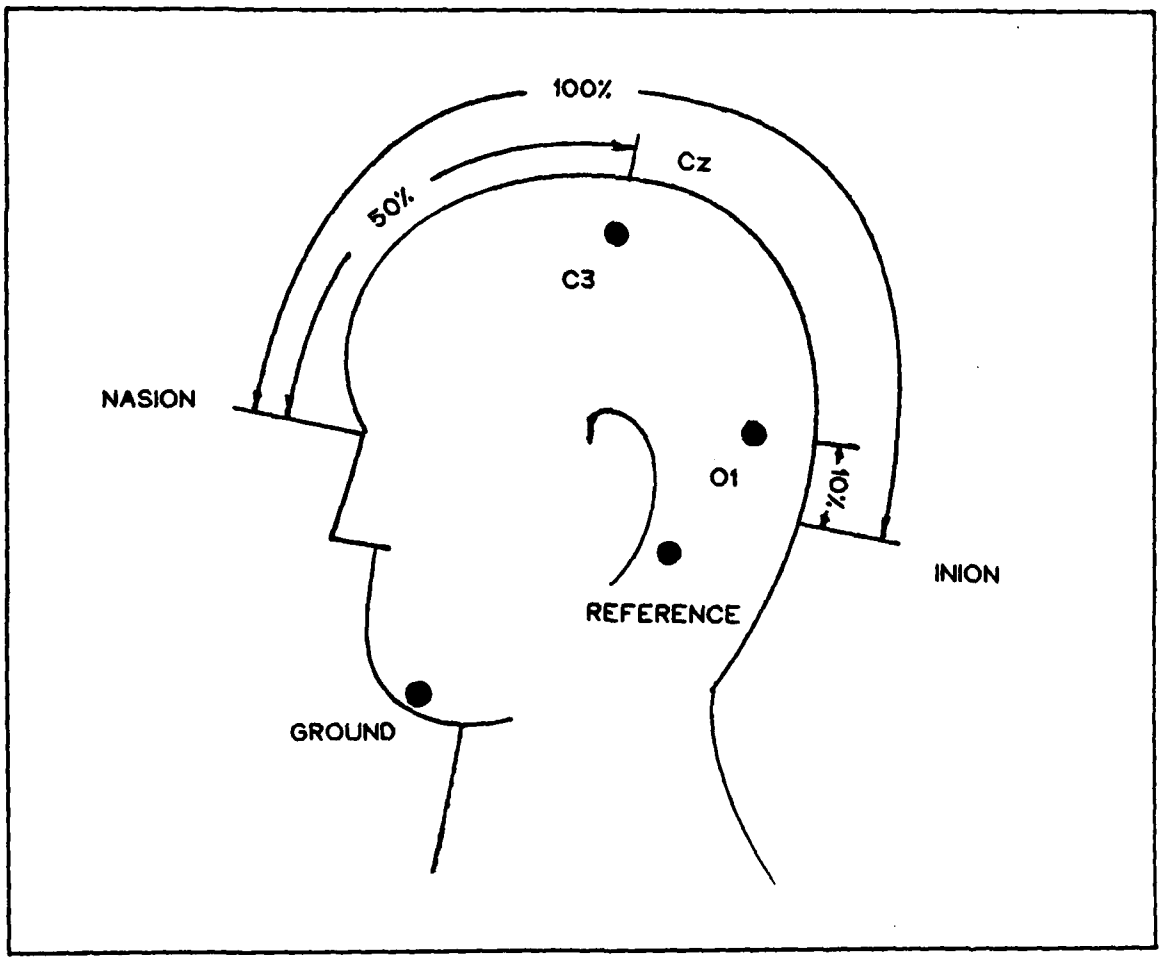

Figure 3.4. Electrode Placement

Data Recording

The output signals from the dc SQUID and the electrodes were fed to an amplifier and bandpass filter (see figure 3.1). The pass band was set between 0.1 and 30 hertz for each channel and the amplification was set at 100 due to the small signal amplitude furnished by the measurement equipment. The amplification factors were included in all calibration calculations. The filtered signals were simultaneously sent to an oscilloscope for real-time monitoring and to the Masscomp 5400 computer for recording. As discussed previously, a timing signal or trigger was supplied to the Masscomp 5400 by the stimulus device.

The Masscomp 5400 Laboratory Computer receives all signals as an analog input. Figure 3.5 shows the signal path within the Masscomp 5400 from the input, where the signals are digitized and multiplexed, to the record device. In this particular case, the MEG signal was processed on channel zero, the EEG on channel one, eye blink data on channel two, and the trigger on channel three. The trigger also supplied timing information to each channel. Both the EEG and MEG signals went through a signal averager which would continuously average the signals over the half second trial interval before plotting them on the screen. The signals were fed simultaneously to an output multiplexer for recording in ASCII format. This final ASCII formatted data, consisting of unaveraged single event evoked responses, was

used exclusively in this experiment. Note the scales on the plot devices: femto-Tesla for MEG signals and micro-Volts for EEG signals. These scales will remain consistent throughout this thesis.

All data collected by the Masscomp 5400 can be stored on magnetic tape. However, for the purposes of processing, the ASCII data for this experiment was transferred to floppy disk for use on a personal computer. Data processing, including signal averaging, signal extraction, spectral densities, and plotting were implemented on The DADiSP Worksheet signal analysis software by DSP Development Corporation.

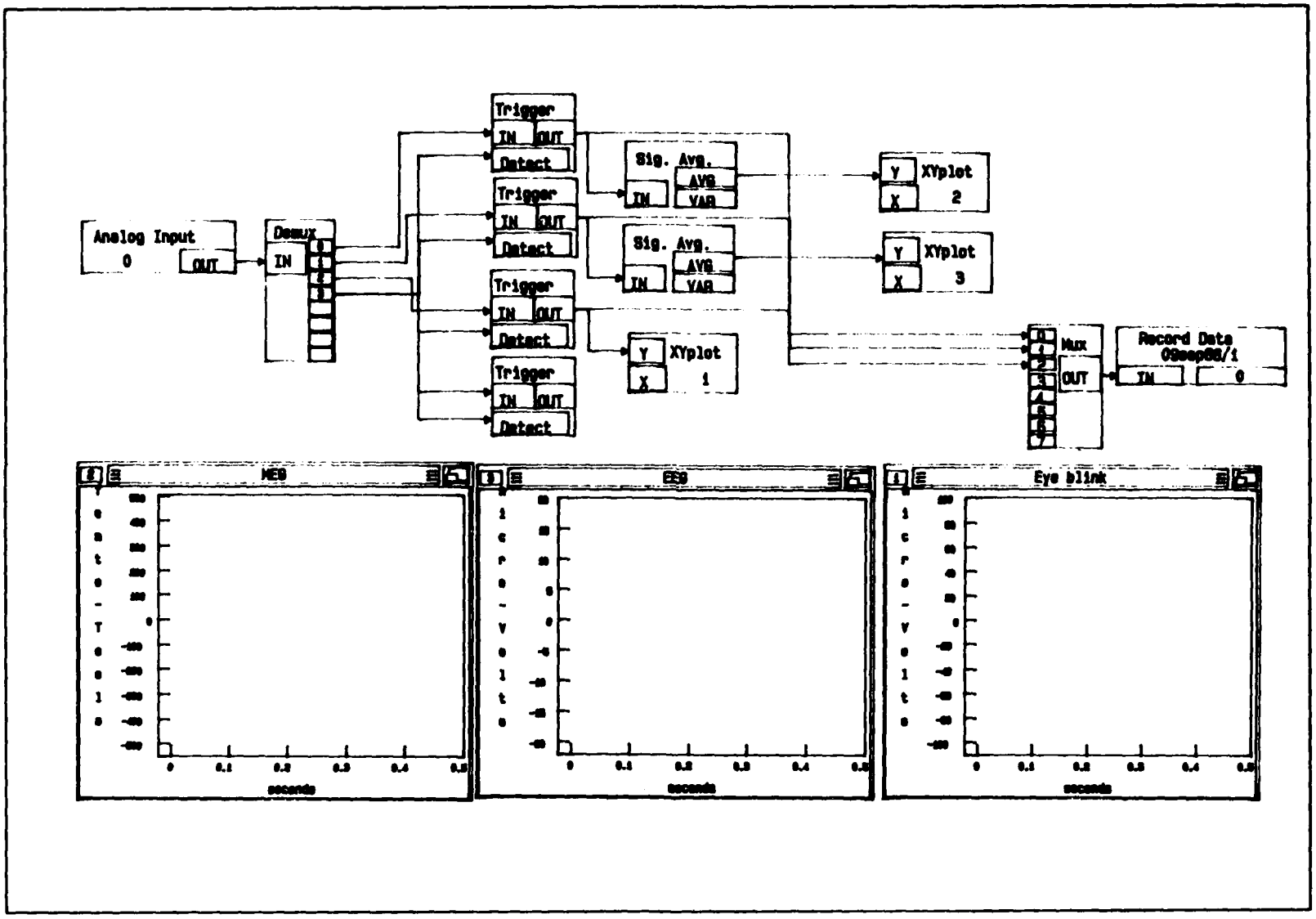

Figure 3.5. Masscomp 5400 Display

IV. Statistical Characteristic and Modeling of MEG and EEG Signals

In order to demonstrate the effectiveness of adaptive processing on ERF and ERP signals, it is first necessary to properly model the evoked fields and potentials that result from a human visual response. Modeling will be based on a statistical analysis of the evoked signals. Investigation of the statistical nature of these signals will include noise characteristics, signal latencies, and spectral content.

Statistical Charateristics

As discussed previously, magnetic field measurements of the brain have shown great promise in localizing specific sources of brain activity. Field measurements resulting from evoked stimuli such as a visual pattern or auditory tone have been used with some success in mapping the locations of where these processes take place within the brain. In studying MEG signals that result from a visual stimulus, the goal is to extract as much information as possible from the portion of the signal produced as a direct result of the stimulus. Accurate extraction of the evoked signal is difficult due to the low signal-to-noise ratio (SNR) caused by various sources of background noise. This background noise is impossible to filter out using linear filtering techniques because much of the background noise

and evoked signal lie within the same signal spectrum. Figure 4.1 shows a typical visual ERF and figure 4.2 shows a background MEG signal of the same length with virtually no stimulus. A comparison of these two signal plots yields a small signal-to-noise ratio.

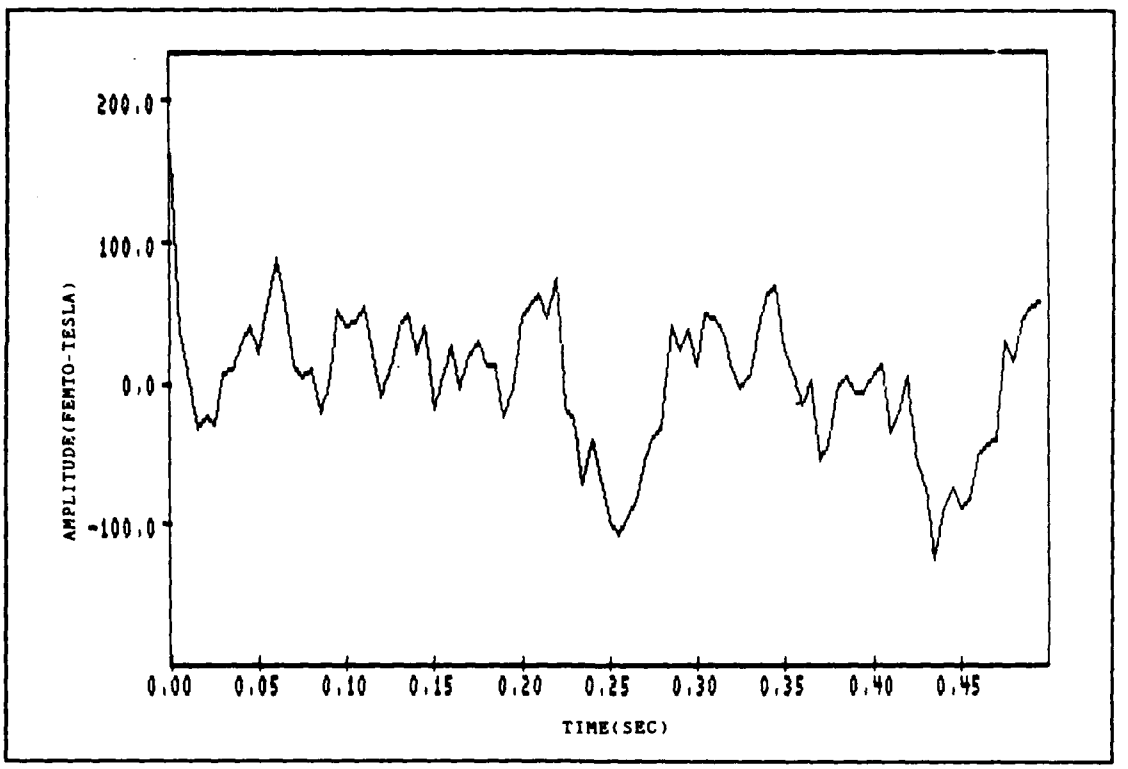

Figure 4.1. Visual ERF Signal

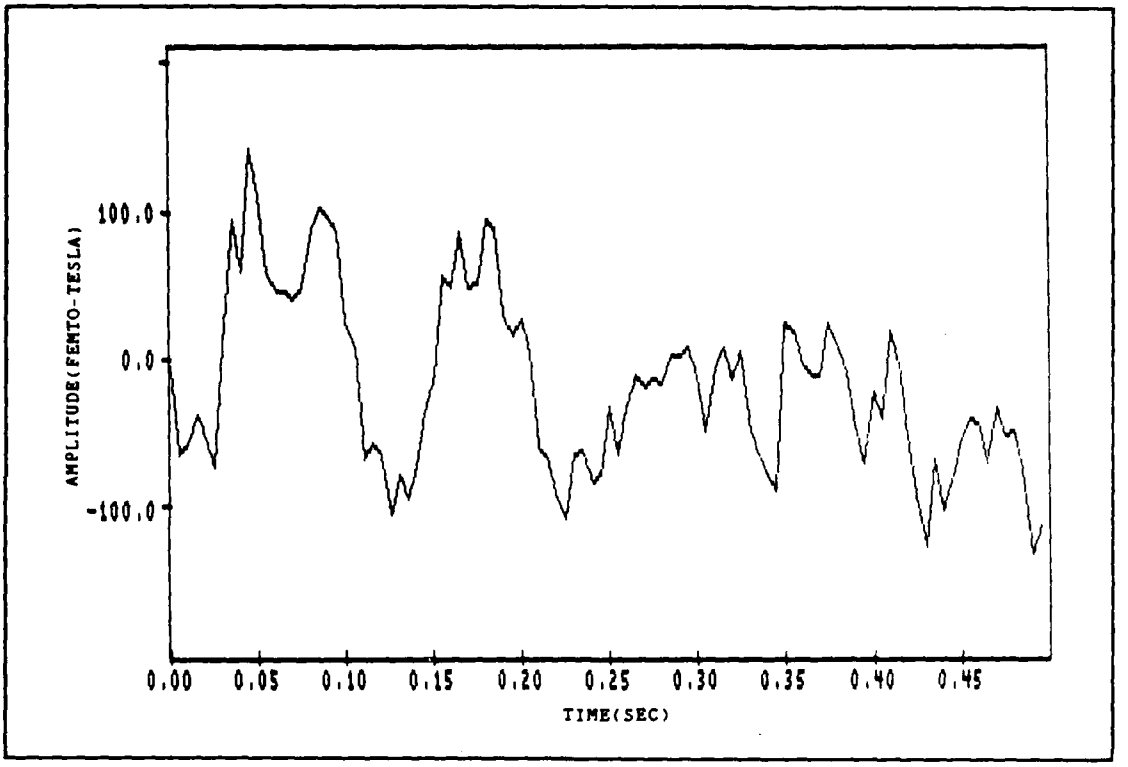

Figure 4.2. No Stimulus MEG Signal

To increase the signal-to-noise ratio of the MEG evoked signal, it is common practice to ensemble average many signals produced from the same stimulus. An improvement in signal-to-noise ratio will result as succesively more ensembles are averaged together. For example, the signal in figure 4.3 shows an ensemble average of 80 visually evoked MEG signals. From this ensemble average, the evoked response can be identified on the plot. (9:8)

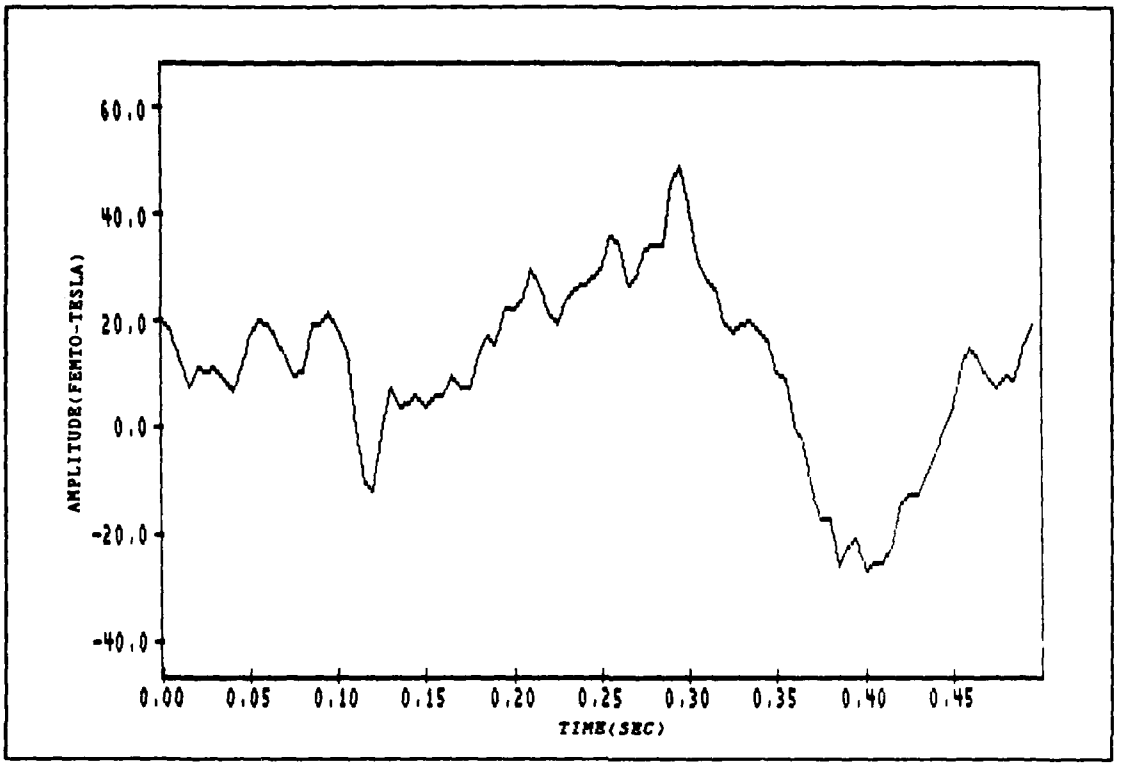

Figure 4.3. Ensemble Average of Evoked Signals

The technique of ensemble averaging is a simple method for improving the SNR of signals. However, several disadvantages become evident when using this technique as a means of improving MEG signal-to-noise ratio. One major disadvantage is the need to average many signals. This requires that the subject be stationary and alert over successive trials of an experiment. This may not seem like a critical problem when recording only 80 separate responses, but the experimental trials add up quickly when doing more complex experiments such as magnetic field

mapping of portions of the brain. Constant repetition of the evoked stimulus may lead to fatigue in the subject and therefore have an impact on the experimental results. A second disadvantage in ensemble averaging is the possible loss of important information. Both the ERF and ERP signals exhibit nonstationary characteristics. During ensemble averaging, these characteristics, in the form of signal latencies, are averaged out of the final resultant signal. Figure 4.4 is an overplot of three separate MEG evoked responses showing the different latencies of each signal.

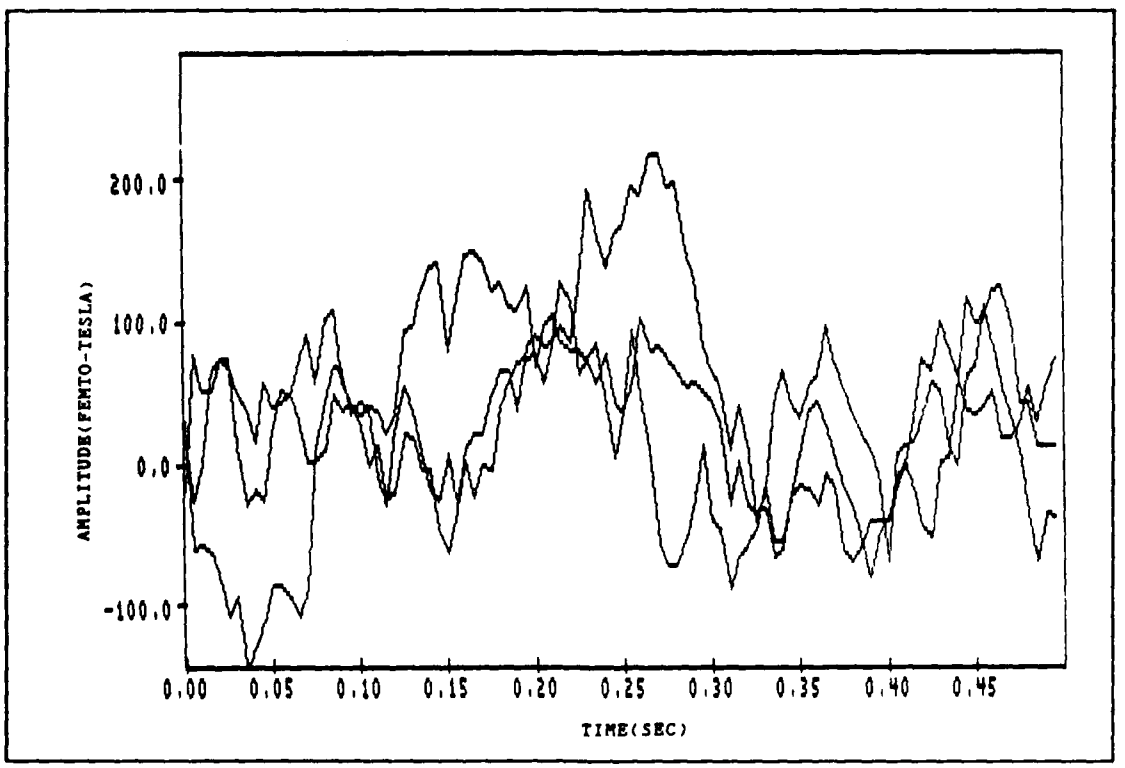

Figure 4.4. ERF Latencies

These latencies may contain important information related to localization or they could be caused by inconsistencies in the test apparatus. In any event, obtaining consistent results over a long period with many experimental trials has proven to be a difficult task. (5:44)

Despite the possibility of losing significant information associated with signal latencies, ensemble averaging still proves to be the best method for determining signal statistics. Generalized evoked stimulus waveforms were obtained by ensemble averaging 80 ERF and ERP signals. An overplot of these two signals is shown in figure 4.5. As discussed in the previous chapter, the scales on the ERF and ERP signals were adjusted to fit the waveforms to the same relative range for plotting. Constant offsets or biases were evident in both ERF and ERP averaged signals for the particular subject data represented in figure 4.5. Using the plotted scale, the ERF averaged signal had a mean of 11.40 and standard deviation of 16.36. The ERP signal mean was -3.58 with a standard deviation of 18.74. The differences in the mean can most likely be attributed to the test apparatus. The mean and standard deviation are used here only to compare the ensemble averaged ERF and ERP signals and do not apply to individual signals because they are non-stationary.

The plots in figure 4.5 show a general similarity to one another in waveform peak locations and waveform periods.

This apparent correlation is even more significant after inverting the ERP signal by multiplying it by negative unity as in figure 4.6. A cross-correlation plot was generated on the ERF and inverted ERP and is shown in figure 4.7. The center peak of this plot represents a maximum correlation. In the following chapter, the apparent correlation of ERF and ERP signals will be further developed as a critical requirement for adaptive filtering. Similar correlation plots were obtained using ensemble averaged audio ERF and ERP data.

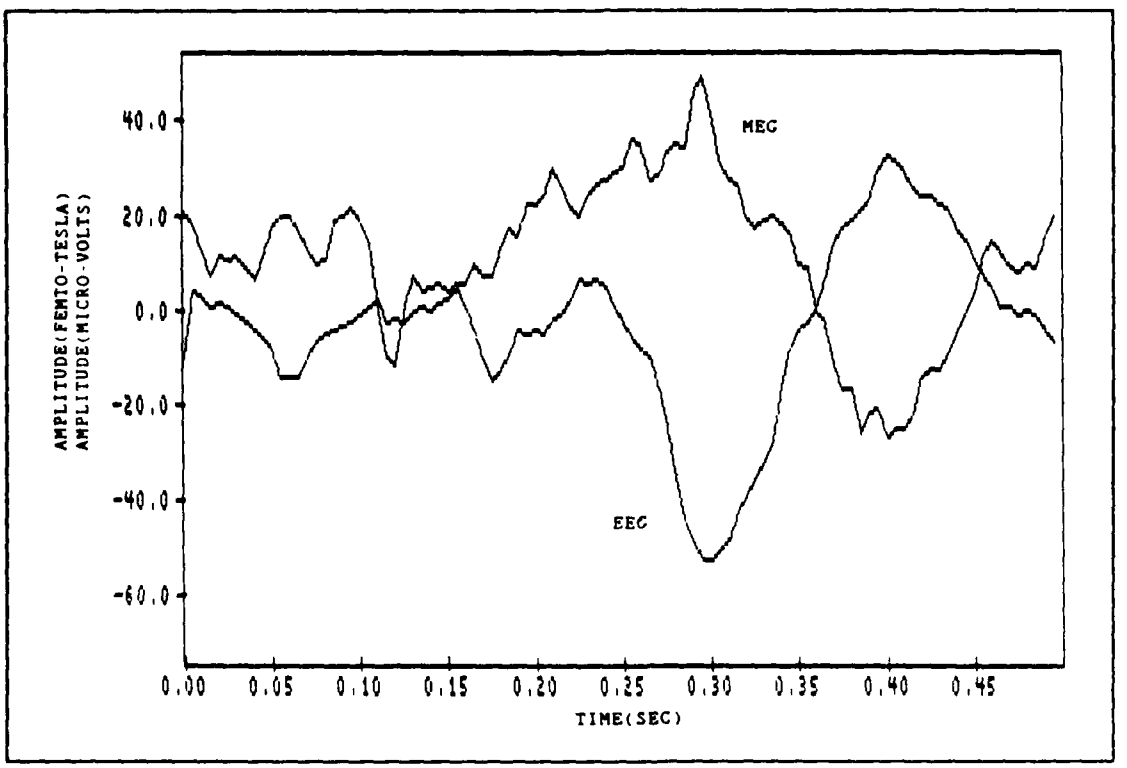

Figure 4.5. ERF and ERP Average Signals

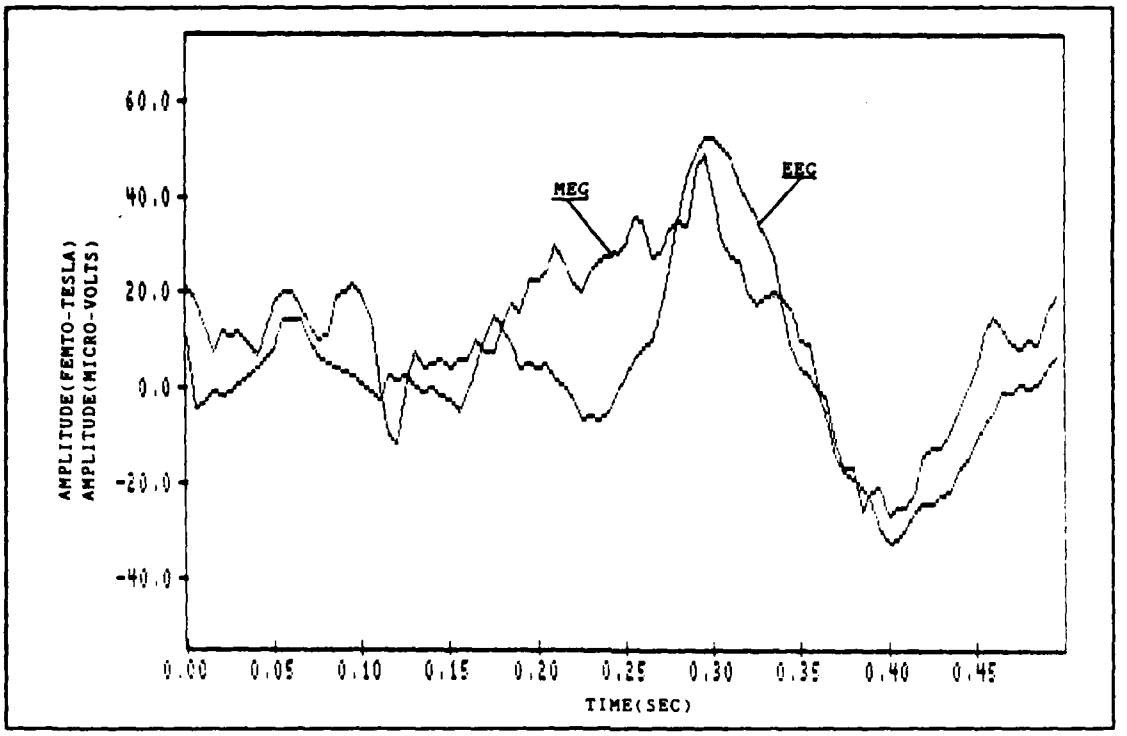

Figure 4.6. ERF and Inverted ERP

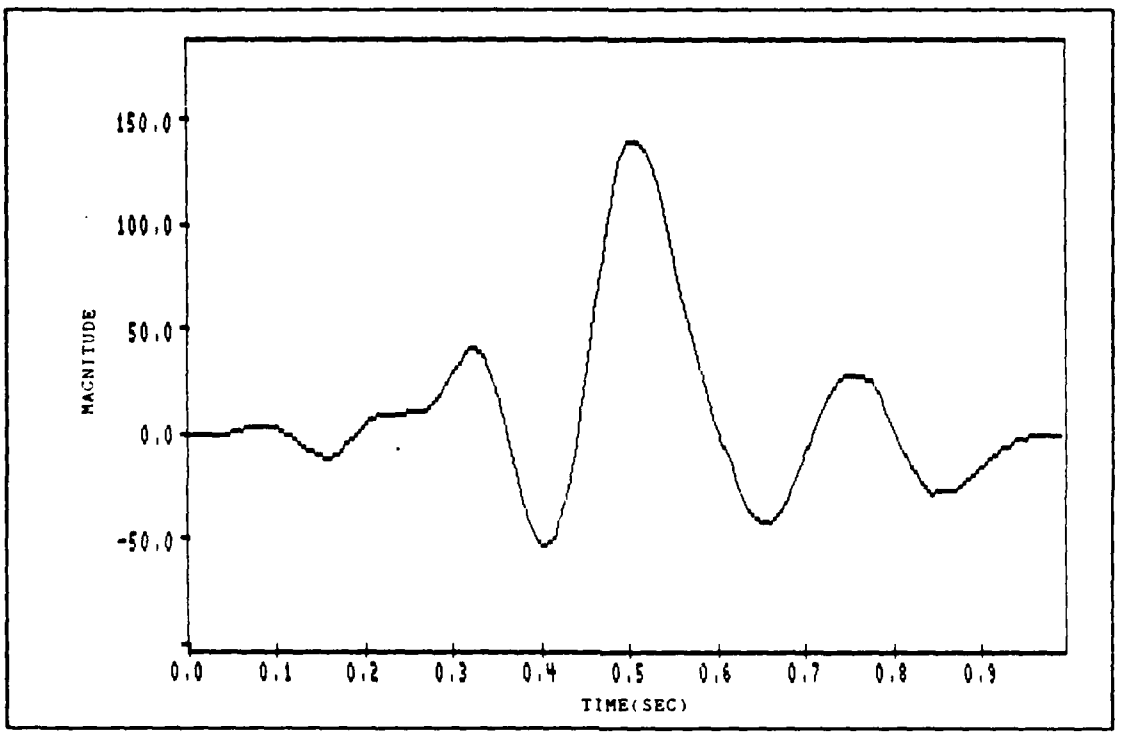

Figure 4.7. Inverted ERP and ERF Cross-correlation

Power spectral densities of the ensemble averaged ERF and ERP signals were analyzed to further verify the similarities between the two signals. Figures 4.8 and 4.9 show the spectral densities of the ERF and ERP ensemble averaged signals. As expected, most of the signal energy in both signals is located at low frequencies (0.5 to 13 hertz). This checks with the frequency ranges presented previously. In this particular case, a major portion of the spectral density in both plots is in the five to six hertz region. Large zero frequency values are ignored as biases in the test apparatus.

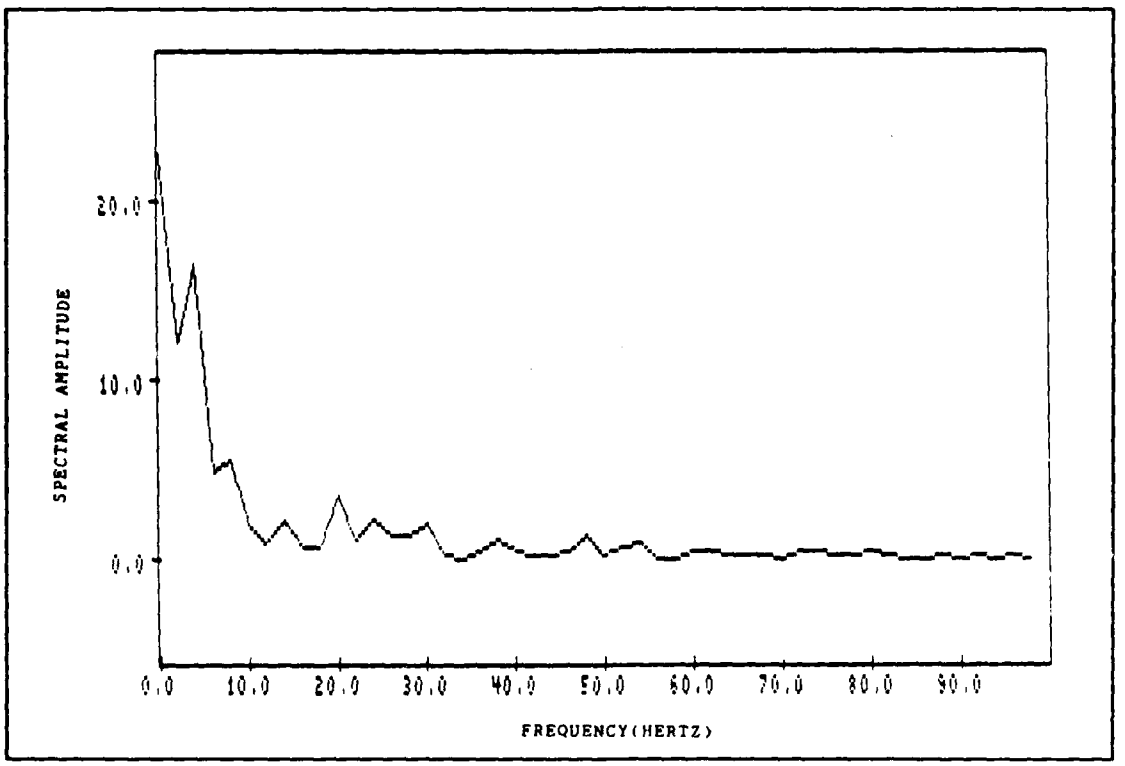

Figure 4.8. MEG Spectral Density

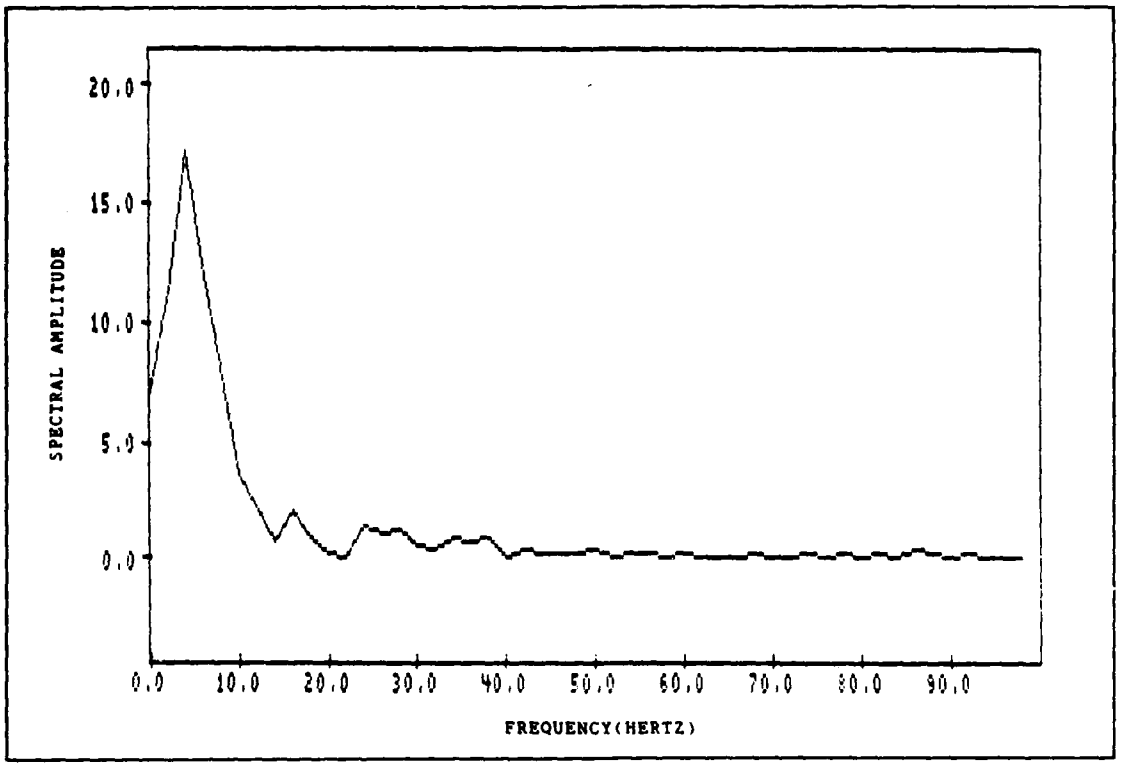

Figure 4.9. EEG Spectral Density

Ensemble averaging has shown several similarities between the ERF and ERP signals. These similarities will be used as a basis for signal modeling and as an important requirement for adaptive processing techniques.

Signal Modeling

For the purposes of analysis, both the ERF and ERP signals will be modeled using a simplified version of the ERP model presented by McGillem and Aunon (8:71-100). Their model can be represented by the following equation:

$$x(t) = \sum_{k=1}^{K} a_k s(t-t_k) \qquad (4.1)$$

where the coefficient a_k and time delay t_k are independent

identically distributed random variables. The function s(t), is a single waveform representing a component of the ERP. The amplitude coefficient and time delay random variables are represented by a gaussian distribution. The waveform components can utilize either gaussian shaped wavelets or a raised cosine pulse. Several models were developed using different latencies and different combinations of waveforms.

In order to maintain a consistent set of data for adaptive processing, a simplified version of the above model will be presented. This model, shown in Figure 4.10, is represented by a full sine wave added to an attenuated half sine wave. The three signal peaks, two positive and one

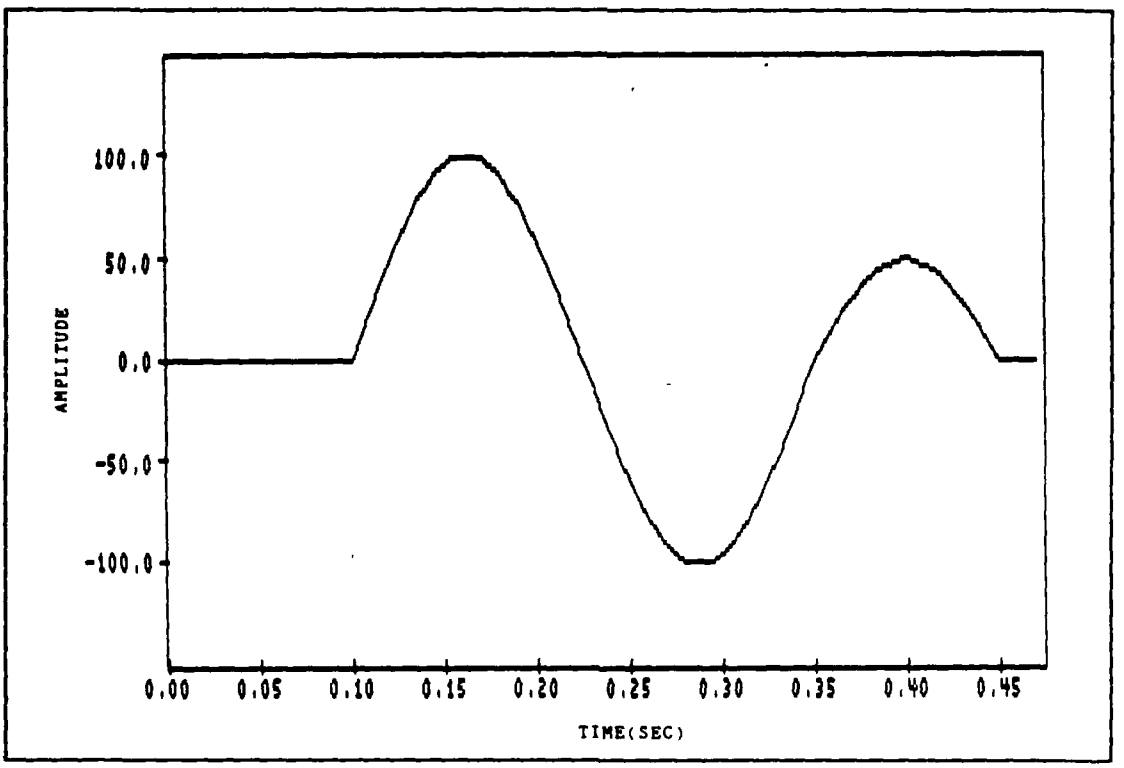

Figure 4.10. Simulated ERP Signal

negative, are consistent with the McGillem and Aunon model (8:92). Independent latencies on each sine wave component are not used on this simplified model. However, the starting point of the total waveform can be adjusted to simulate signal latencies as shown in Figure 4.11. This same basic model has been used in previous ERP signal processing studies by Thakor (9:8) and Yu (16:735).

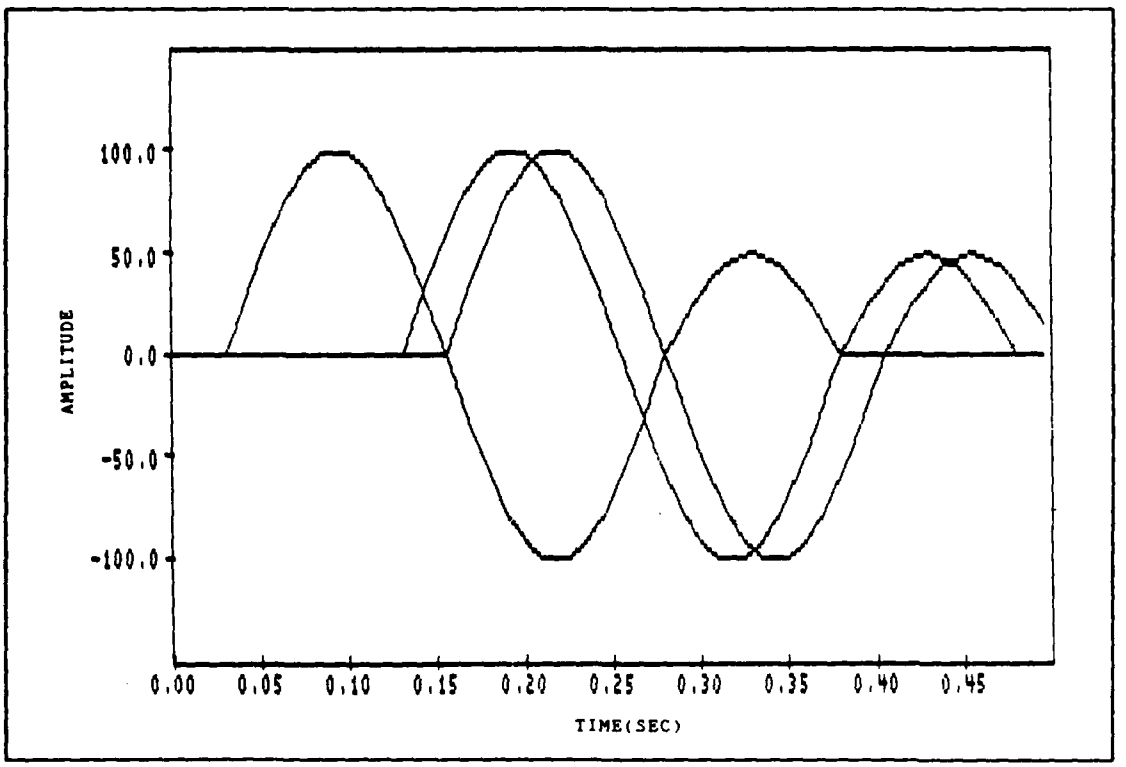

Figure 4.11. Simulated ERP Signals With Latencies

The similarities between the ERP and ERF signals discussed previously serve as a basis for using the same model for both signals. The ERP signal can be inverted by multiplying by negative unity to more realistically simulate the waveform in Figure 4.5. With the addition of white gaussian noise, the generalized signal waveform is defined (see figure 4.12).

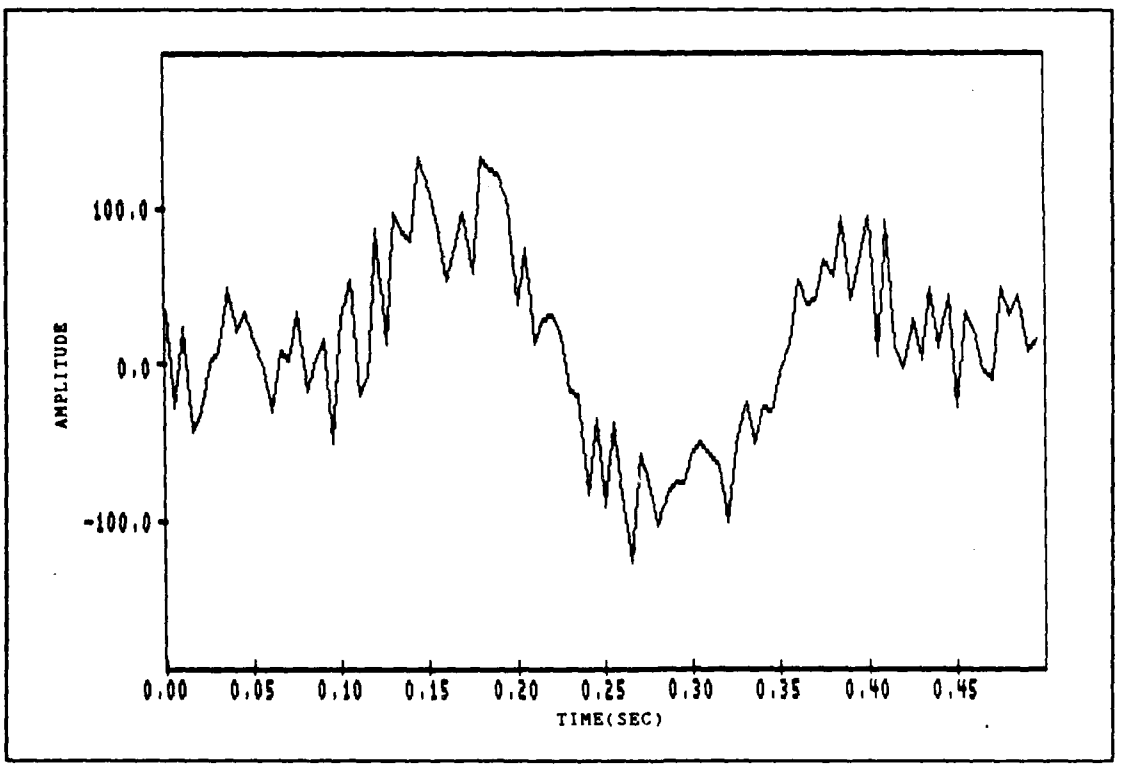

Figure 4.12. Generalized Model Plus Noise

V. ADAPTIVE FILTER IMPLEMENTATION

This chapter will discuss the filtering of ERF signals using the ERP as a reference signal. A simplified model of this adaptive process will be presented along with a description of the computer program that actually processes the signals of interest. The adaptation process will first be discussed in terms of the signal model presented in Chapter IV. Adaptive filtering using human visual and audio evoked responses will follow. Additionally, each filter output sample, using either modeled or human data, will be analyzed to determine its validity.

Signal Source and Adaptive Processing Model

As discussed previously in Chapter II, adaptive signal processesing is implemented using a signal enhancing version of the adaptive filter shown in figure 2.4. Further definition of the signal enhancing model as applied to ERF and ERP signals is shown in figure 5.1. In this model, the ERF plus MEG signal is designated as the desired signal (d). The ERP plus EEG is the input to the adaptive processor (x). The output of the adaptive processor (y) is subtracted from the desired signal to obtain the error signal (ε). In theory, the adaptive processor output should converge to a signal similar to the desired signal minus the noise as the

error signal approaches zero. As figure 5.1 indicates, all input signals originate within the human brain and some correlation exists between the ERP and the ERF. Noise due to the measurement equipment such as the SQUID, electrodes, and bandpass filter, is also indicated in figure 5.1. However, to simplify the signal model, these noise sources were assumed to be small compared to the EEG and MEG and were therefore neglected.

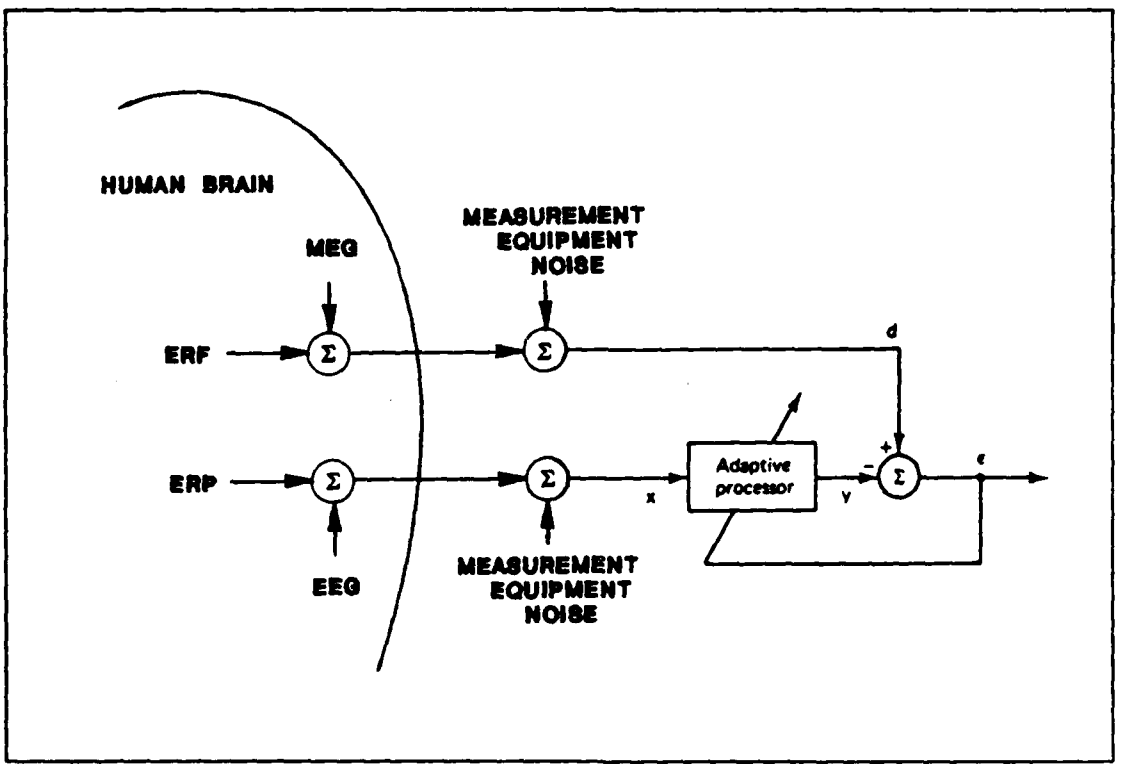

Figure 5.1. Signal Source and Adaptive Model

Adaptive Filter Program

As discussed in Chapter II, adaptive processing of the ERP and ERF was implemented using the least-mean-square

(LMS) adaptive algorithm. As stated previously, an error signal, ε, is determined by subtracting the output of the adaptive processor from the desired signal (the ERF in this case). This was given in Chapter II as

$$\varepsilon(k) = d(k) - \underline{W}(k)^T \underline{X}(k) \qquad (2.5)$$

where $\underline{W}(k)$ is the weight vector at time k, and $\underline{X}(k)$ is the input vector at time k. The LMS algorithm utilizes the error signal and the input signal to continuously update the weights using the following equation:

$$\underline{W}(k+1) = \underline{W}(k) + 2\mu\varepsilon(k)\underline{X}(k) \qquad (2.16)$$

where 2μ is a convergence factor.

The above algorithm was implemented on a personal computer using the Turbo-Pascal programming language by Borland. A listing of this program is located in Appendix A. To simplify data processing, this adaptive filtering program was converted to an executable file for utilization as a stand alone program. It is capable of handling up to 8000 data points with up to 50 weights. Input data files, called from disk drive A, must be designated as "meg.dat" and "eeg.dat" which represent the ERF signal and ERP signal respectively. The data run number, μ (the convergence factor with limits of 0.0 to 1.0), and filter size, are entered at the keyboard. The filter output and error signals are displayed on the computer monitor and saved on disk drive A.

Adaptive Processing Using Modeled Signals

To demonstrate that the LMS program operated properly and that adaptive processing is a plausible method of ERF noise filtering, a series of experiments using modeled data was undertaken. The following list describes each experiment:

(1) The same signal plus random noise was applied to both the desired input and reference input.

(2) Two different signals plus noise were applied to the inputs. The waveforms of the two signals were the same but the desired input signal waveforms are negative while the reference input is positive. Additionally, waveform latencies were random.

(3) This experiment was similar to Experiment Two except that both inputs were positive. Again, waveform latencies were random.

(4) The signals in this experiment were the same as those used in Experiment Three but with a delay added to the reference input signal.

(5) The desired signal and reference signal were correlated as in Experiment One. However, in this experiment, human MEG and EEG background signals were added to the model instead of random noise.

Experiment One. The purpose of this experiment was to insure that the LMS program could filter the random noise associated with the desired signal and reference signal. The noise added to each signal was not correlated. The two filter input signals were exactly the same before the noise was added and consisted of five concatenated versions of the signal model presented in Chapter IV. This model is shown in figure 5.2. Notice that the signal amplitude is normal-

ized as will be all subsequent signal amplitudes presented in this chapter. Figure 5.3 shows the same signal as in figure 5.1 with random noise added. The amplitude of the random noise was also normalized before adding it to the modeled signal. A signal-to-noise ratio of unity was therefore obtained.

The two signals plus noise, representing both the desired signal input and the reference signal input, were applied to the LMS filter using a convergence factor, μ, of 0.005 and a filter size consisting of 20 weights. Choice of these parameters was based on the following equations and actual filter output results (12:211):

$$M \approx \frac{n}{N} \tag{5.1}$$

and

$$0 < \mu < \frac{1}{n \cdot (\text{signal power})} \tag{5.2}$$

where

M = filter misadjustment
n = number of weights or filter size
N = number of training samples.

Misadjustment is defined by Widrow as "a measure of how closely the adaptive process tracks the true Wiener solution (11:110)." A typical value for many engineering problems is 10%; however, the above equations apply up to a misadjustment value of 25% (13:1155). Using a misadjustment value of 10% in equation 5.1 with the number of training samples

equal to 100, the number of weights required in the adaptive filter is 10. Using this number in equation 5.2, the upper limit for the convergence factor is found to be 0.1 (signal power for the normalized signal is one). The value of μ used in the filter is typically on the order of 10% of the upper limit (11:106).

Using the values obtained from 5.1 and 5.2 as a baseline, the Experiment One data model was run through the filter. After several data runs, it was found that optimum filtering of the model occurred using 20 weights with a convergence factor of 0.005. Both values meet the requirements of equations 5.1 and 5.2.

Results of Experiment One are shown in figures 5.4 and 5.5. Figure 5.4 shows the filter output while figure 5.5 is an overplot of the input reference signal and the filter output. It can be seen from figure 5.5 that a significant amount of noise was filtered from the input signal. This is also shown in figure 5.6, an error plot generated by subtracting the filter output from the desired signal waveform model and squaring the result. Notice that the error starts off fairly large at the beginning of each 0.5 second response and decreases until the beginning of the next response. This illustrates the adaptive process as it converges to a minimum error. The non-stationary nature of the signal forces the adaptive processor to continuously search for the minimum error.

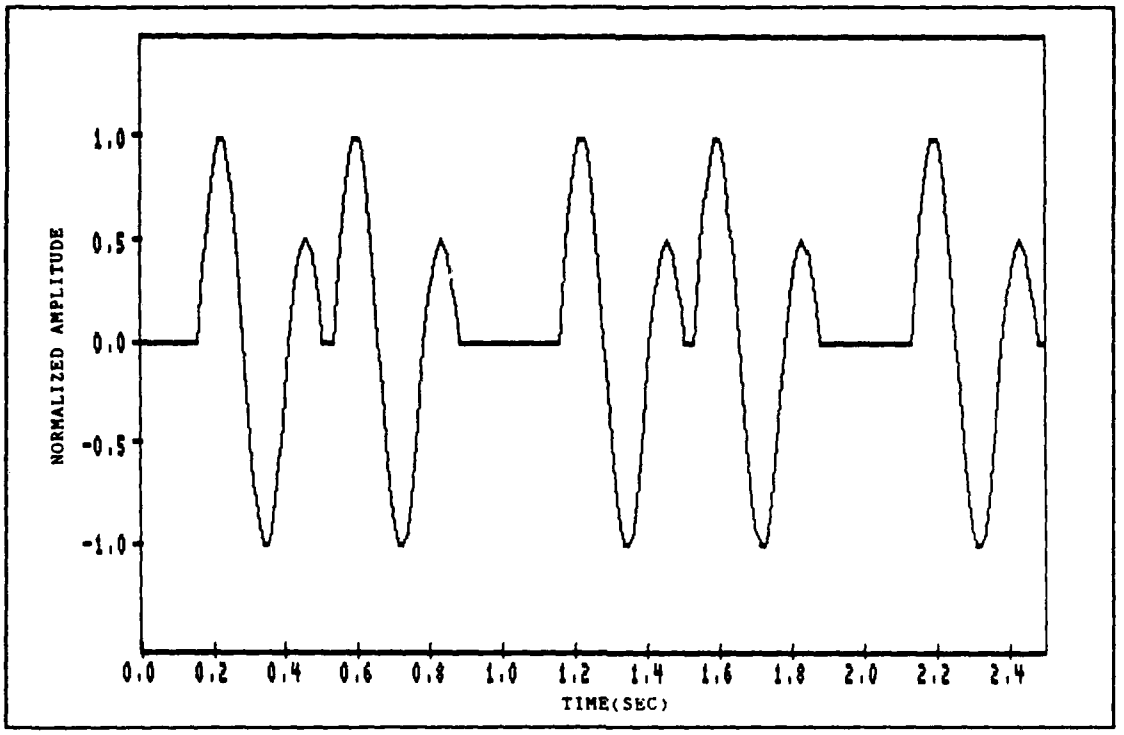

Figure 5.2. Signal Model for Experiment One

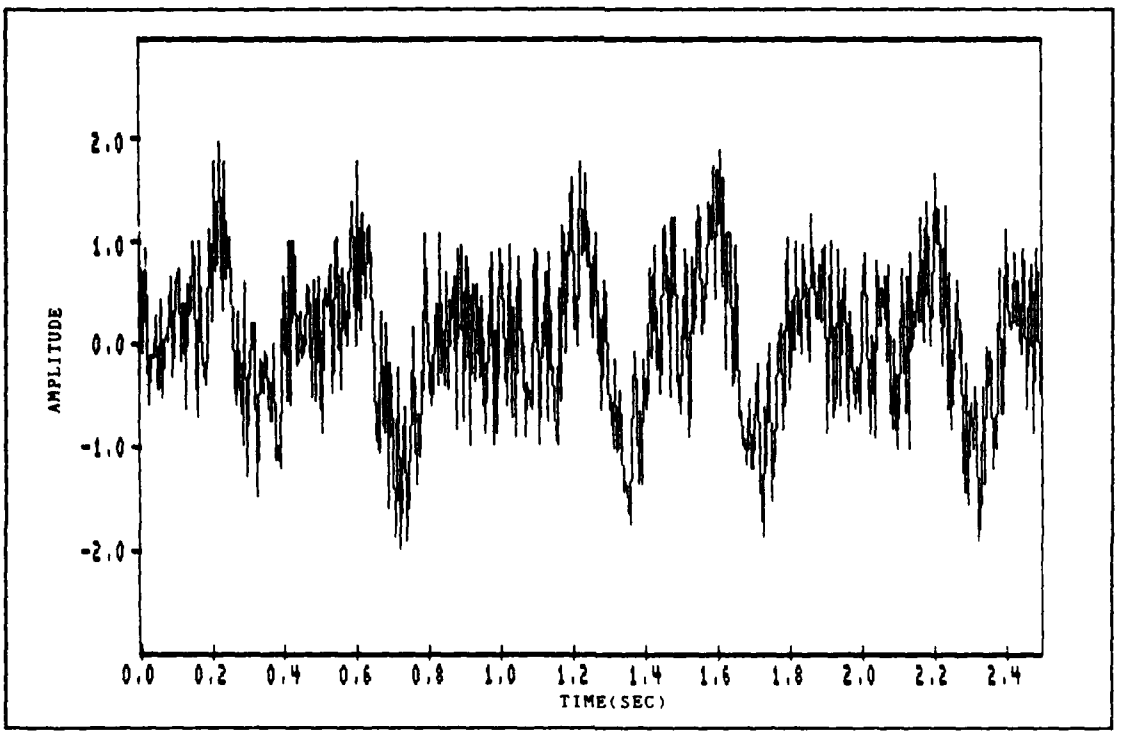

Figure 5.3. Experiment One Signal and Noise Model

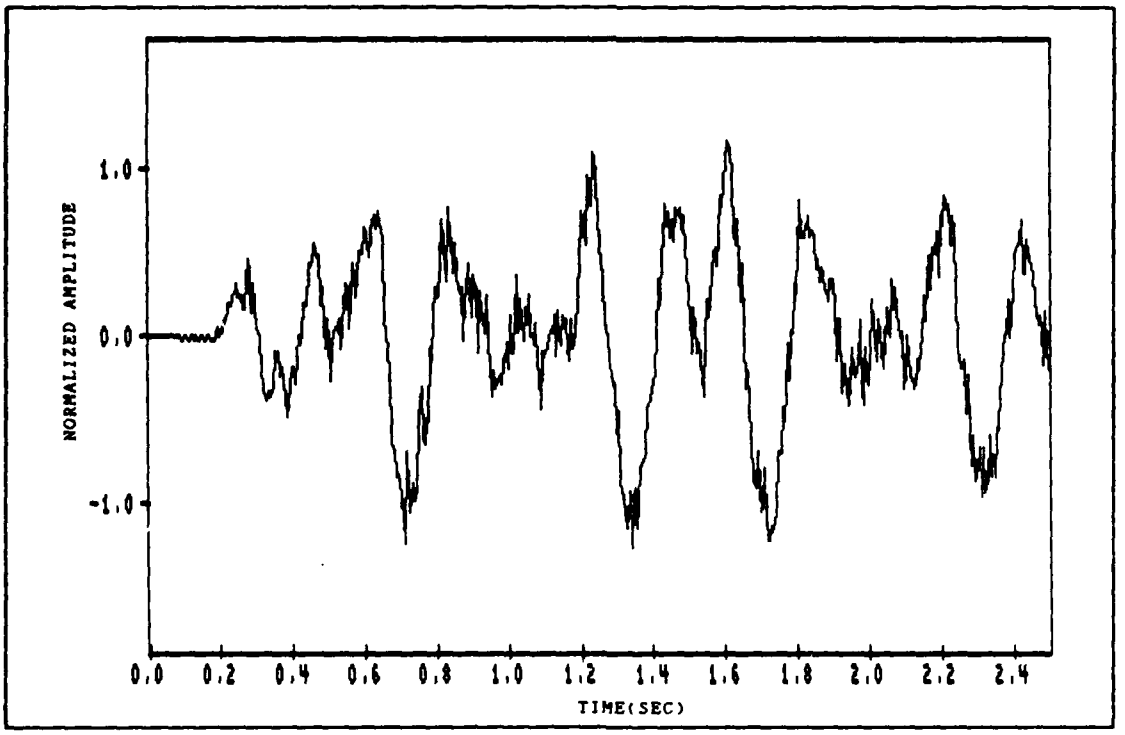

Figure 5.4. Experiment One Signal Output

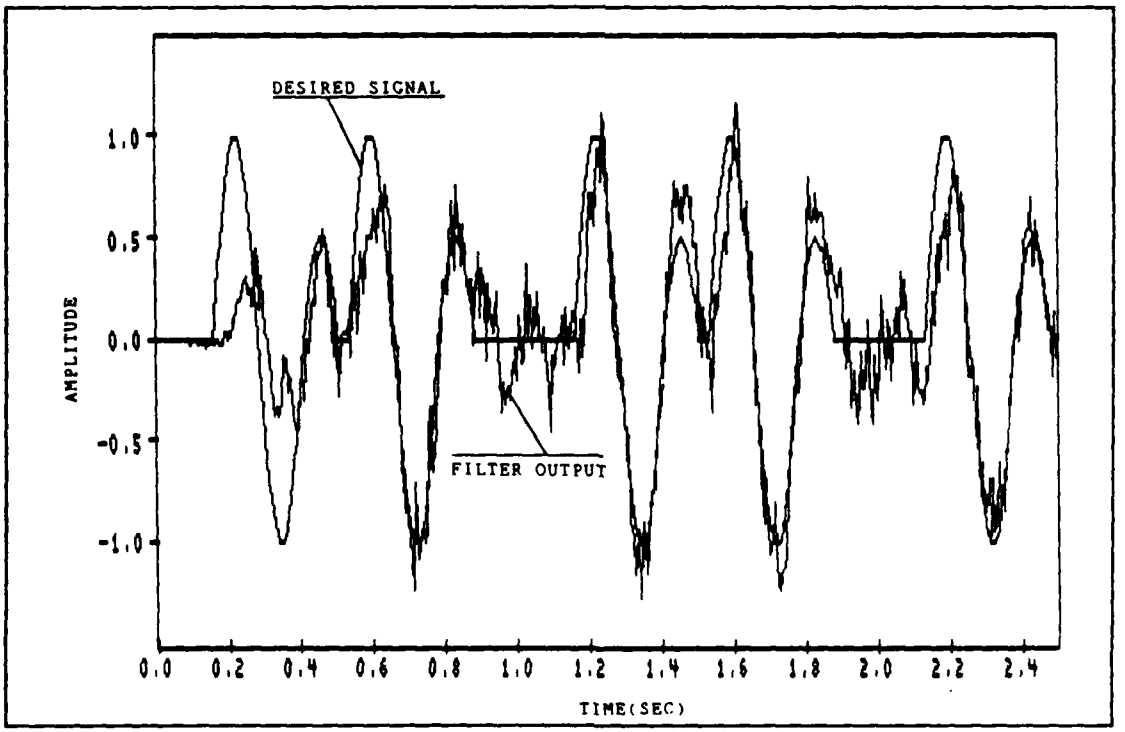

Figure 5.5. Experiment One Model and Output

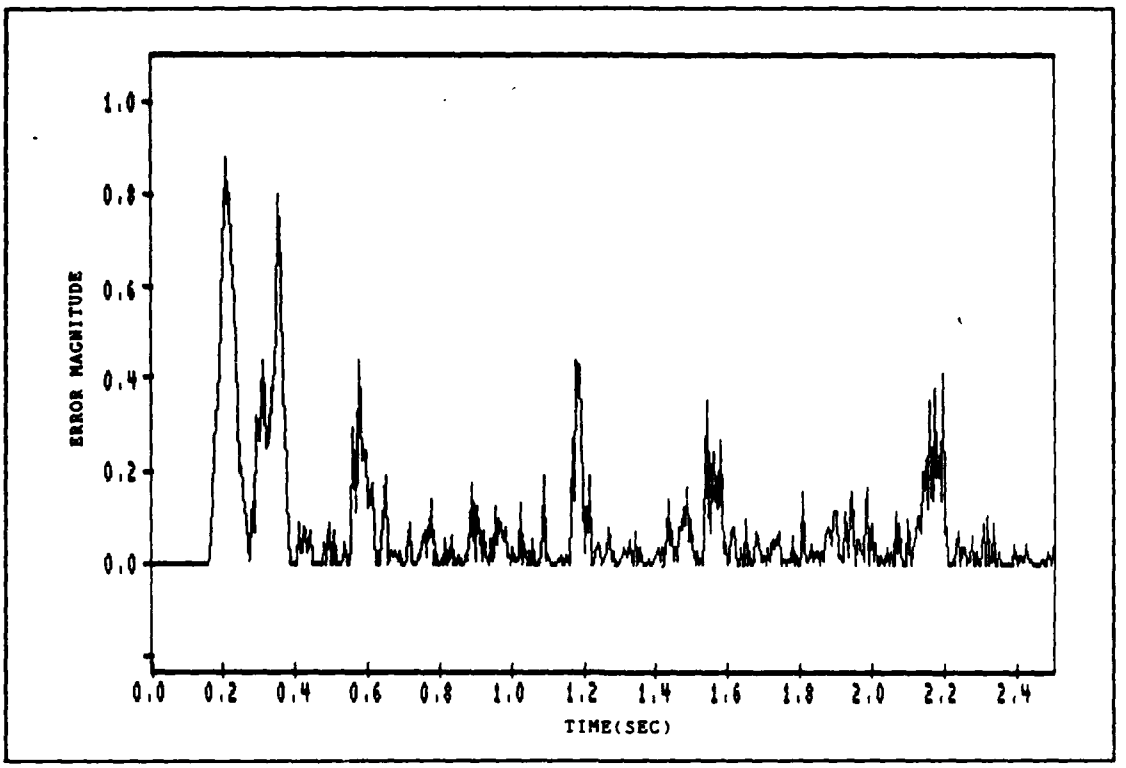

Figure 5.6 Experiment One Error Magnitude

Experiment Two. This experiment was designed to represent the non-stationary nature exhibited by the ERP and ERF signals. The desired signal, representing five ERF signals plus noise with random latencies for each signal, is the same as that of Experiment One. This signal is shown in figure 5.7. The filter input signal also consists of five separate signals and represents the ERP. However, unlike Experiment One, the reference input signal latencies do not necessarily match those of the desired signal. Additionally, each ERP signal is a negative representation of the model presented in Chapter IV (see figure 5.8). This corresponds to a negative correlation between the desired signal,

the ERF, and the reference input signal, the ERP.

The filter size and convergence factor for Experiment Two were the same as that of Experiment One. The filter output signal is shown in figure 5.9 with an overplot of the output signal and reference signal shown in figure 5.10. Notice that the signal waveform features evident in the Experiment One output signal are more difficult to pick out in the Experiment Two output. It is apparent that the adaptive process is complicated by the differences in signal latencies between the reference signal and the input signal. Additionally, the negative correlation resulted in a slight delay in the output and a noticeable phase difference between the output and the reference signal. The error magnitude signal is shown in figure 5.11. As in Experiment One, the large error peaks coincide with the starting point of the first waveform in each of the five responses. In most cases, the error decreases until the beginning of the next response waveform. The error magnitude of each response is dependent on the correlation between the desired signal and the reference input. A rapidly decreasing error curve is evident when there is good correlation.

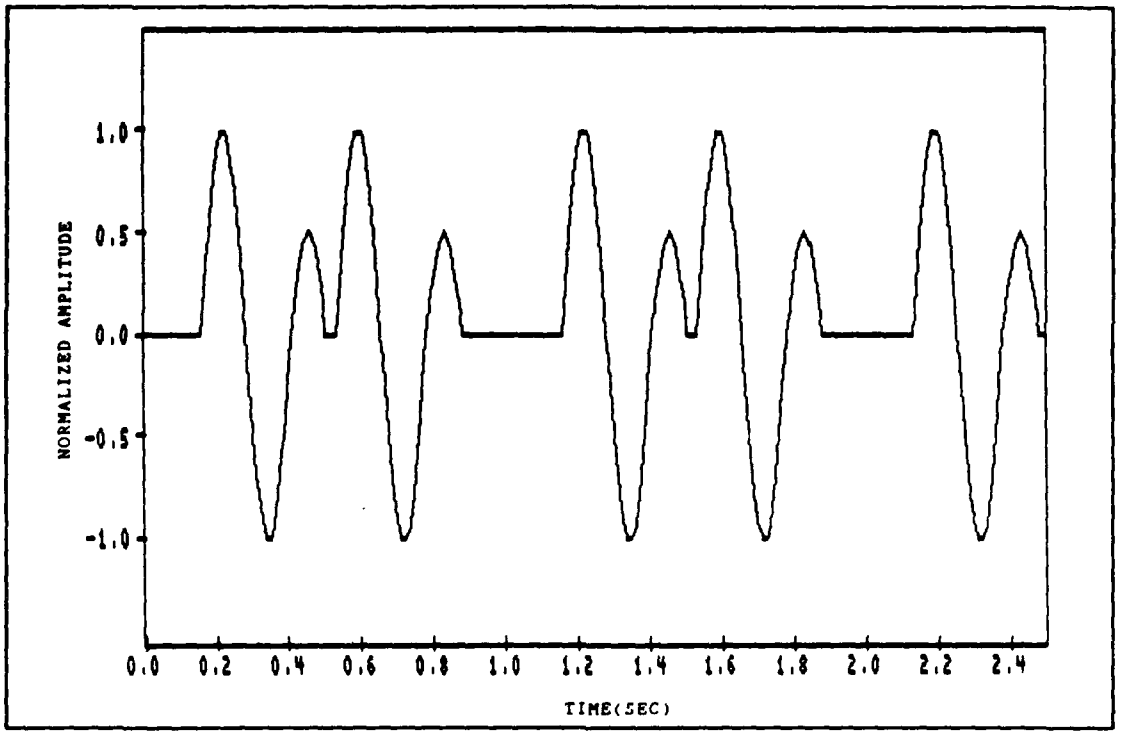

Figure 5.7. Experiment Two Desired Signal

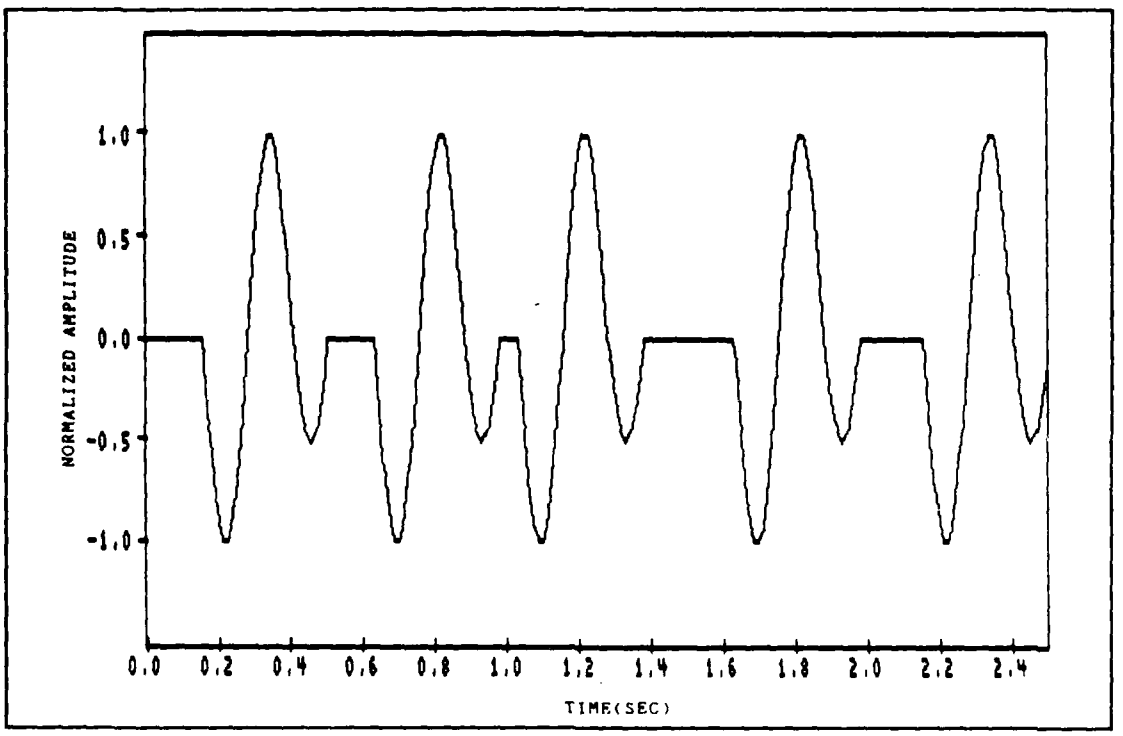

Figure 5.8. Experiment Two Reference Input Signal

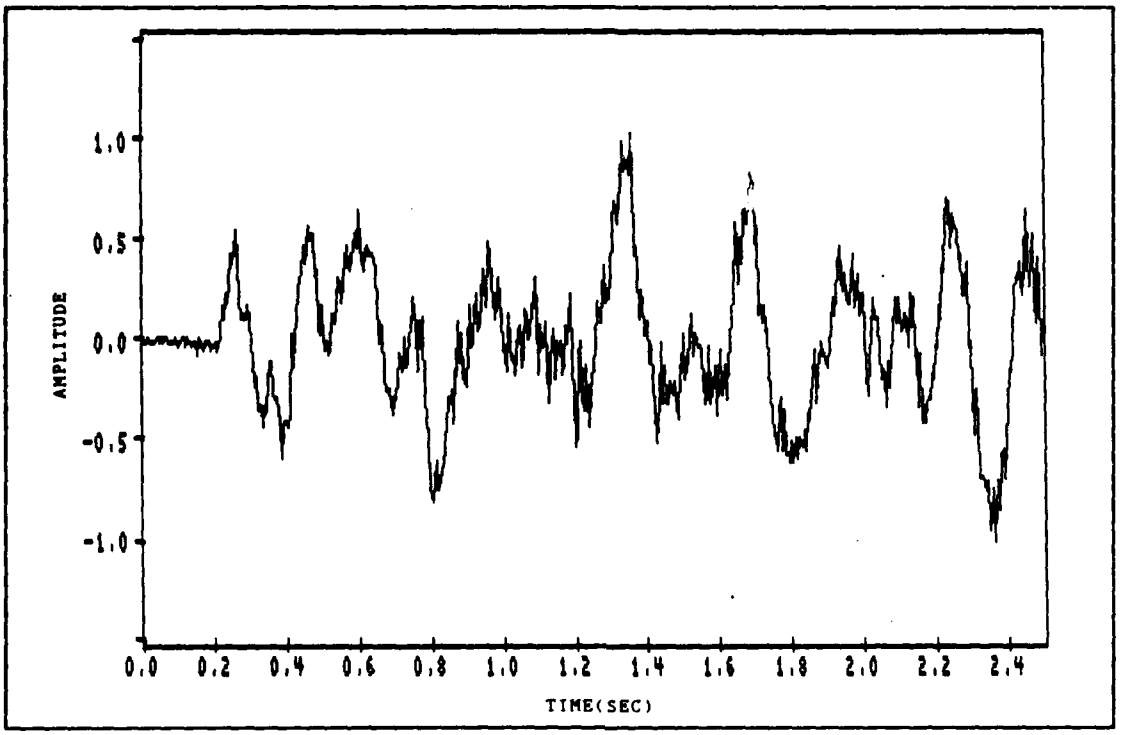

Figure 5.9. Experiment Two Output Signal

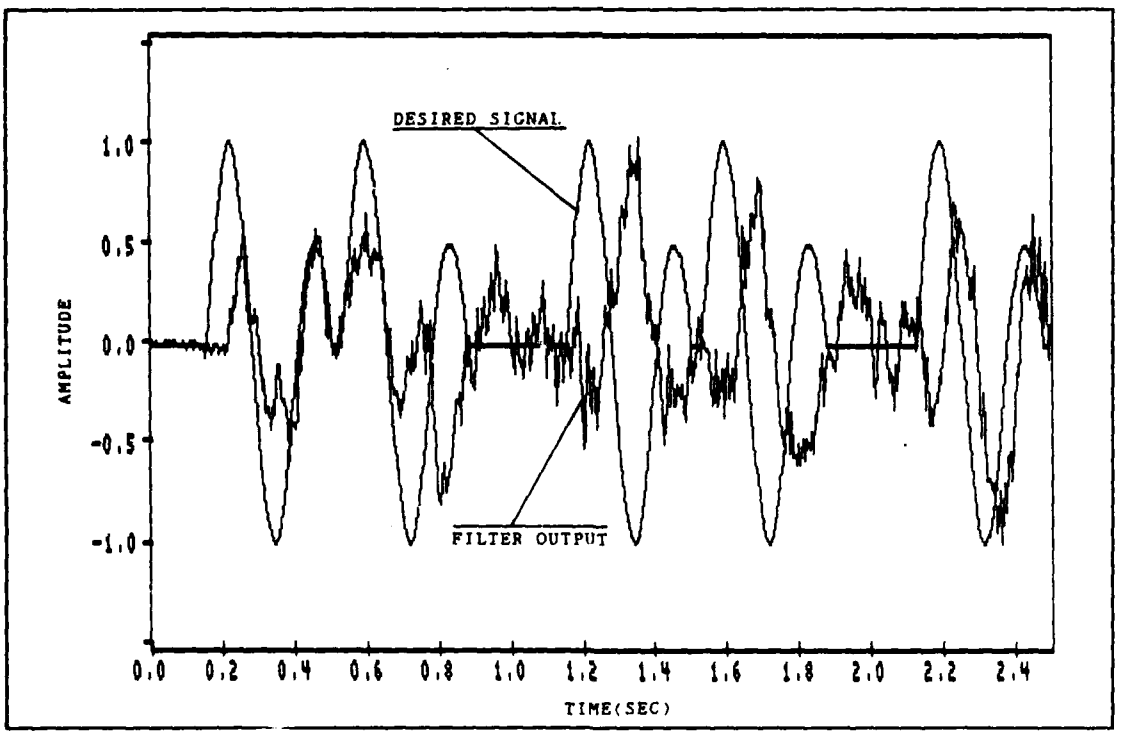

Figure 5.10. Experiment Two Output Signal and Model

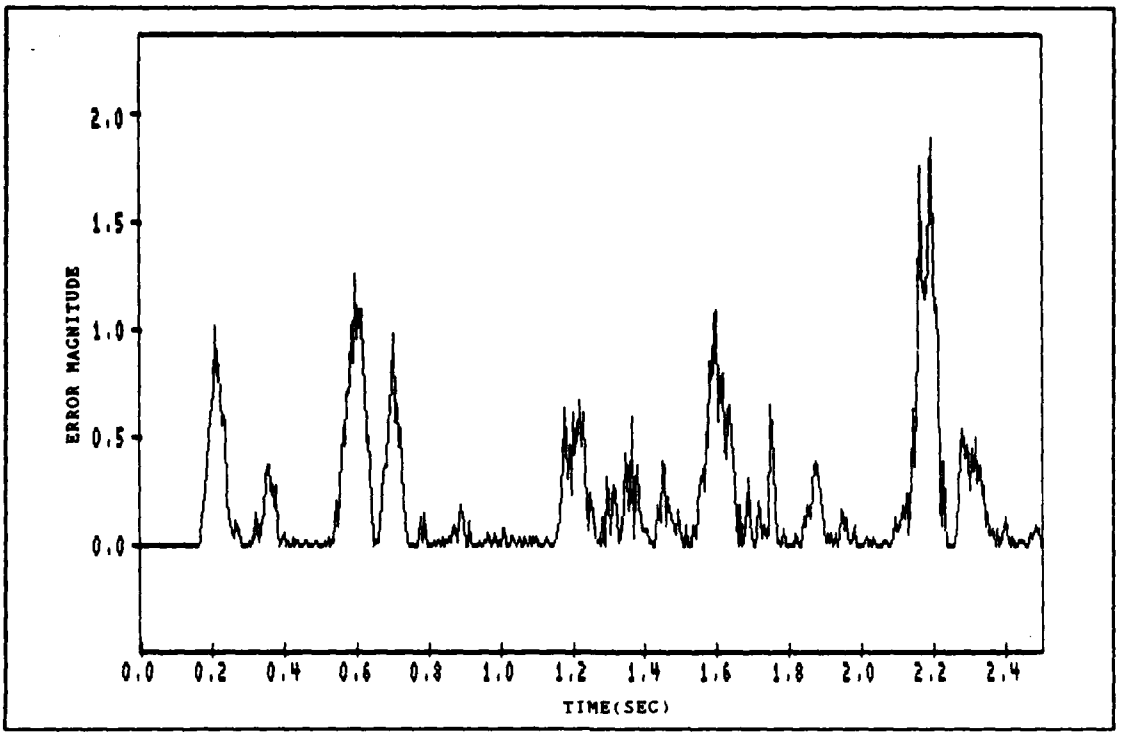

Figure 5.11. Experiment Two Error Magnitude

Experiment Three. As in Experiment Two, both the desired signal and the reference input signal had random latencies. In this experiment, however, the filter input signal was multiplied by negative unity to obtain a positive correlation between the input signal and the reference signal (see figure 4.6). This was done in order to speed up the adaptation process by minimizing the processing delay caused by negative correlation between the desired and reference signals. Previous tests on the LMS adaptive filter using a sine wave as the desired input and a phase shifted sine wave as the reference input had shown that an decrease in the phase offset between the two inputs resulted

in a decrease in filter convergence time. This idea was extended to the signals in this experiment, where there is essentially a 180° phase shift between signals.

The filter size was again 20 weights with a convergence factor of 0.005. Figure 5.12 is a plot of the output signal and figure 5.13 shows an overplot of the output signal and the filter reference signal. Some of the phase shift due to processing delay has been reduced and most signal peaks are clearly evident in figure 5.13. However, the third large positive signal peak is difficult to differentiate from the noise. This can be explained by comparing the reference input signal to the desired signal. A very large latency difference exists between the second and third signal model of the filter input. The correlation between the two signals is very small during this time period resulting in a loss of signal information. This lack of correlation also shows up as an increase in the error signal magnitude (see figure 5.14). A comparison of the error magnitude with that of the Experiment Two error magnitude does not show a clear improvement in the filter output signal for each of the five responses after multiplying the reference signal by negative unity. As in Experiment Two, large errors are evident at the beginning of each individual response and decrease until the beginning of the next response as the adaptation process converges.

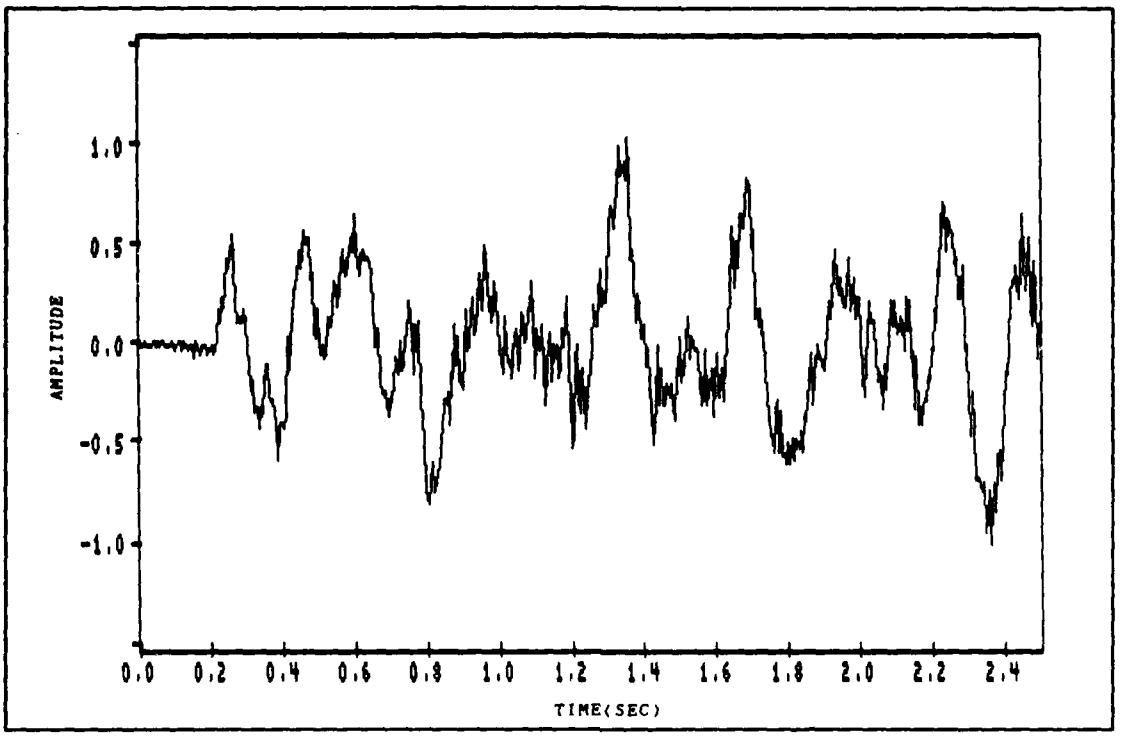

Figure 5.12. Experiment Three Output Signal

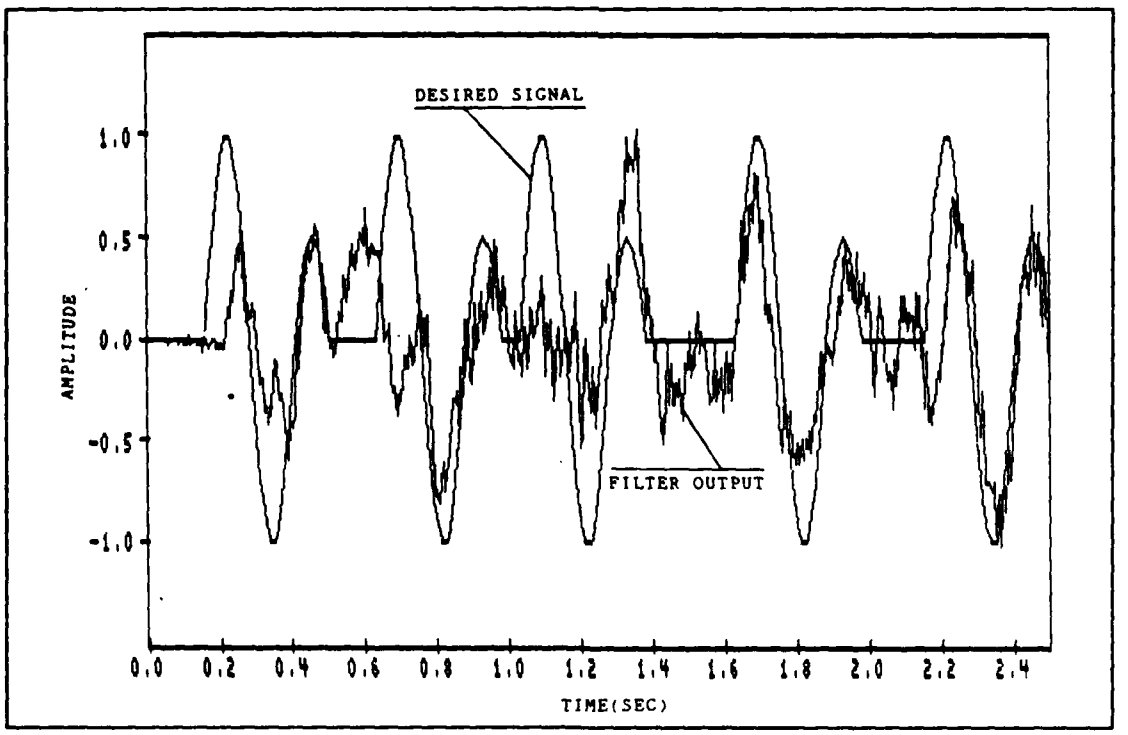

Figure 5.13. Experiment Three Desired and Output Signals

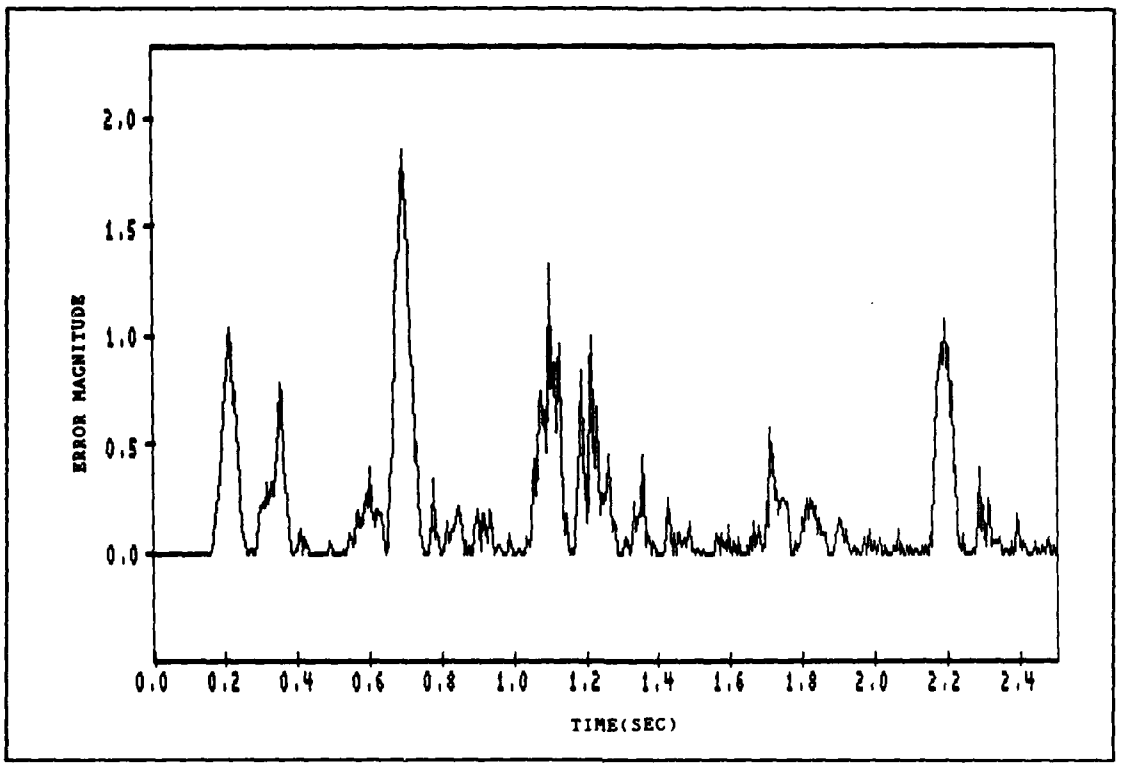

Figure 5.14. Experiment Three Error Magnitude

Experiment Four. This experiment was designed to take advantage of a delay in the desired signal to make the impulse response of the filter causal and physically realizable. All conditions of Experiment Three were repeated except a delay of half the filter size (10 data points in this case) was added to the beginning of the desired signal. The size of the delay is chosen such that the peak of the impulse response will be centered along the delay line of the adaptive filter. (11:325)

Figure 5.15 is a plot of the Experiment Four output signal and figure 5.16 shows an overplot of the output signal with the desired signal. All signal peaks can be

seen in figure 5.16 but a large phase delay exists between the two signals. The phase delay also substantially increases the error signal magnitude as shown in figure 5.17. Any advantage gained in waveform identification using the delay technique of this experiment is offset by the large phase delay of the output. This technique was therefore not used on human data.

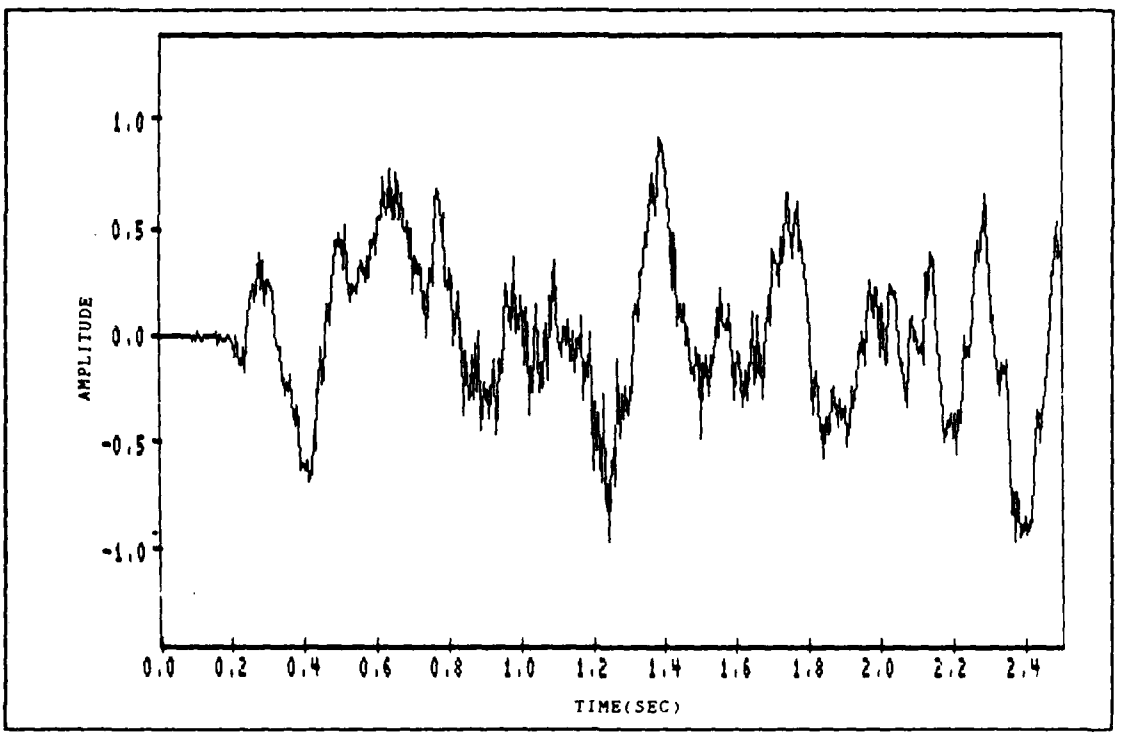

Figure 5.15. Experiment Four Output Signal

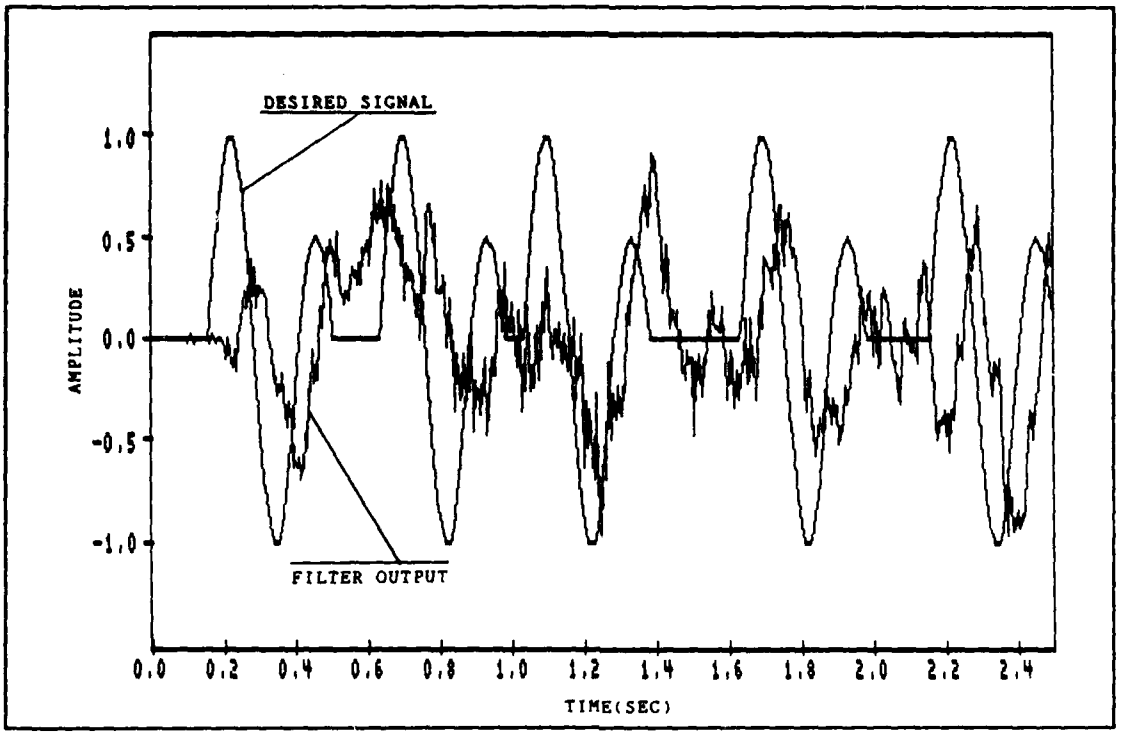

Figure 5.16. Experiment Four Output and Desired Signals

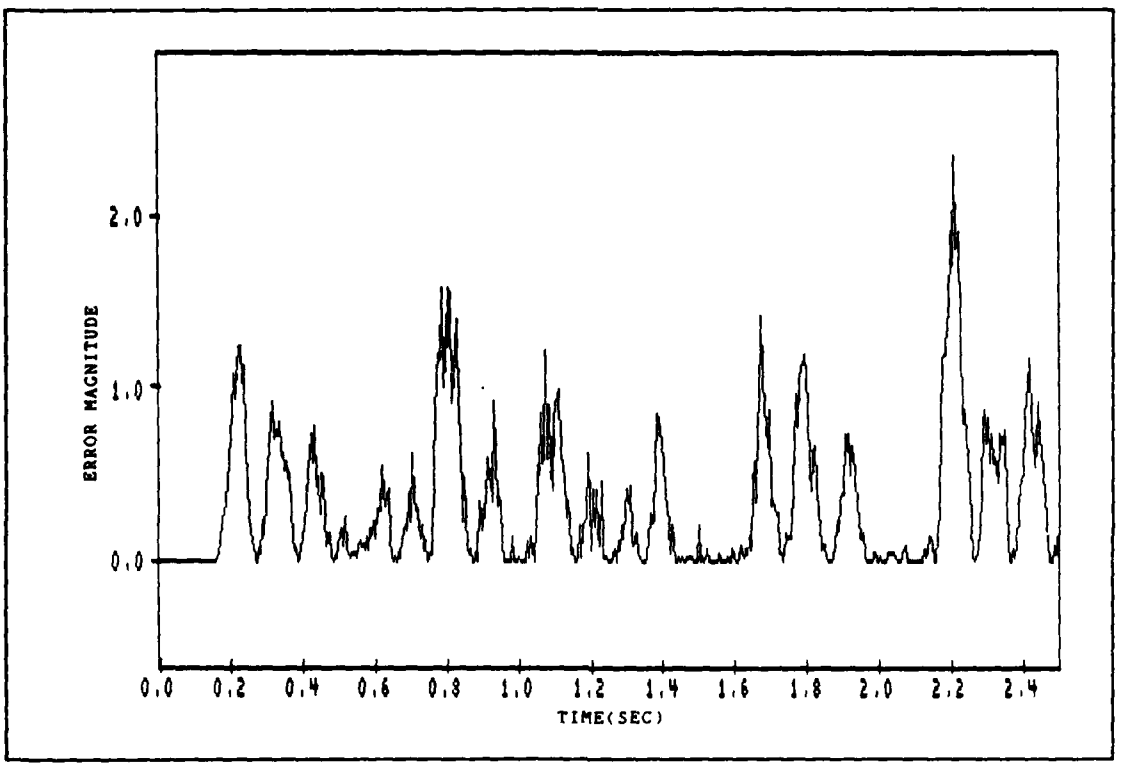

Figure 5.17. Experiment Four Error Magnitude

Experiment Five. The objective of this research is to improve the ERF signal detection when it is degraded by background MEG. This final experimental effort therefore, was designed to test the adaptive filter using a modeled ERF signal corrupted by human background MEG.

Correlated signals representing the ERF and ERP were added to the MEG and EEG respectively. Figure 5.18 shows the normalized ERF model corrupted by the normalized MEG by adding the two signals together. The EEG signal, which was added to the ERP, was not correlated with the MEG signal. As in the previous experiments, the modeled ERF plus MEG was applied to the desired signal input of the filter and the modeled ERP plus EEG was applied to the filter's reference input. The output of the filter is shown in figure 5.19 with an overplot of the desired signal. The error magnitude between the non-corrupted desired signal and filter output is shown in figure 5.20. After initial adaptation of the filter, the error decreased and stayed fairly constant over each of the responses. A large error on the last response can be explained by examining the desired input signal in figure 5.18. The last ERF signal, at around the 2.3 second point on the plot, added to a background signal of approximately the same duration and frequency. The addition of these two signals was subsequently enhanced by the filter resulting in a waveform with a higher amplitude than the original desired waveform.

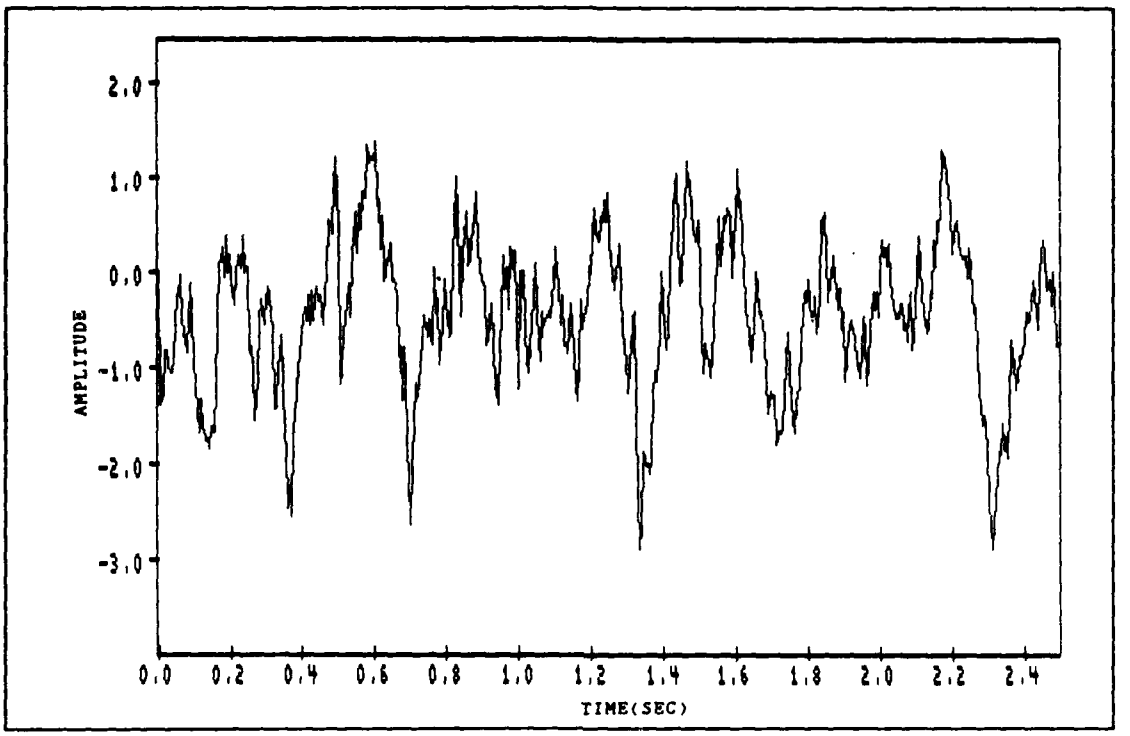

Figure 5.18. Experiment Five Desired Signal Plus Noise

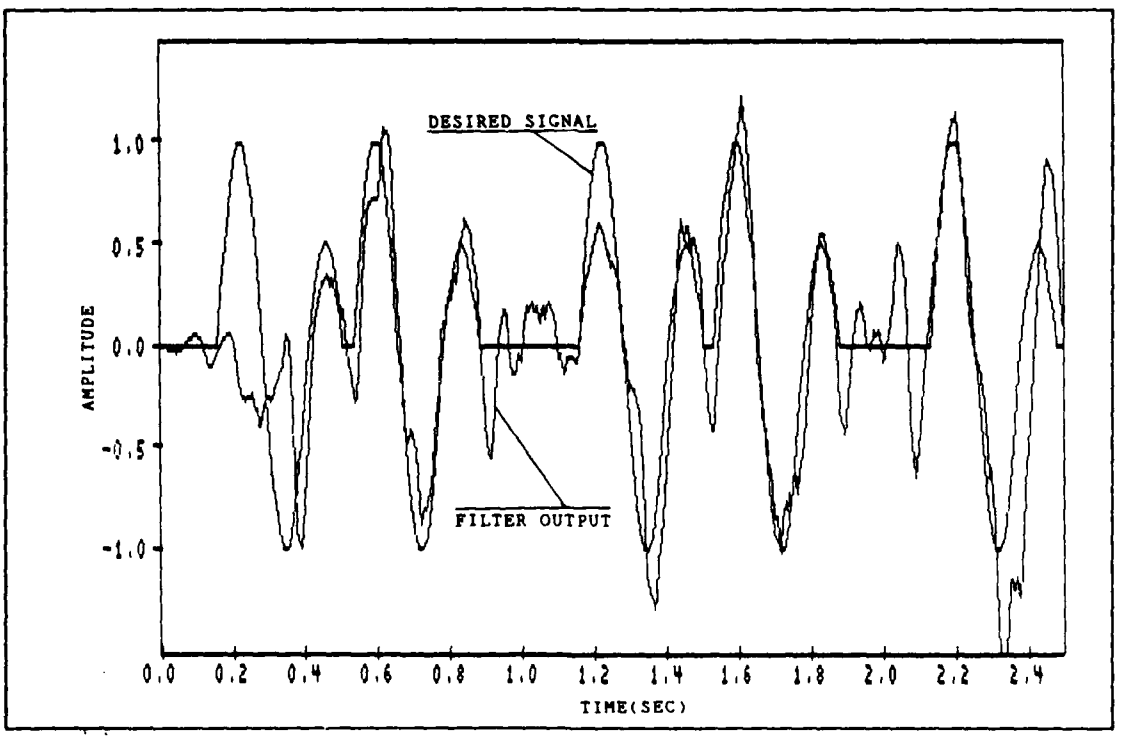

Figure 5.19. Experiment Five Output and Desired Signal

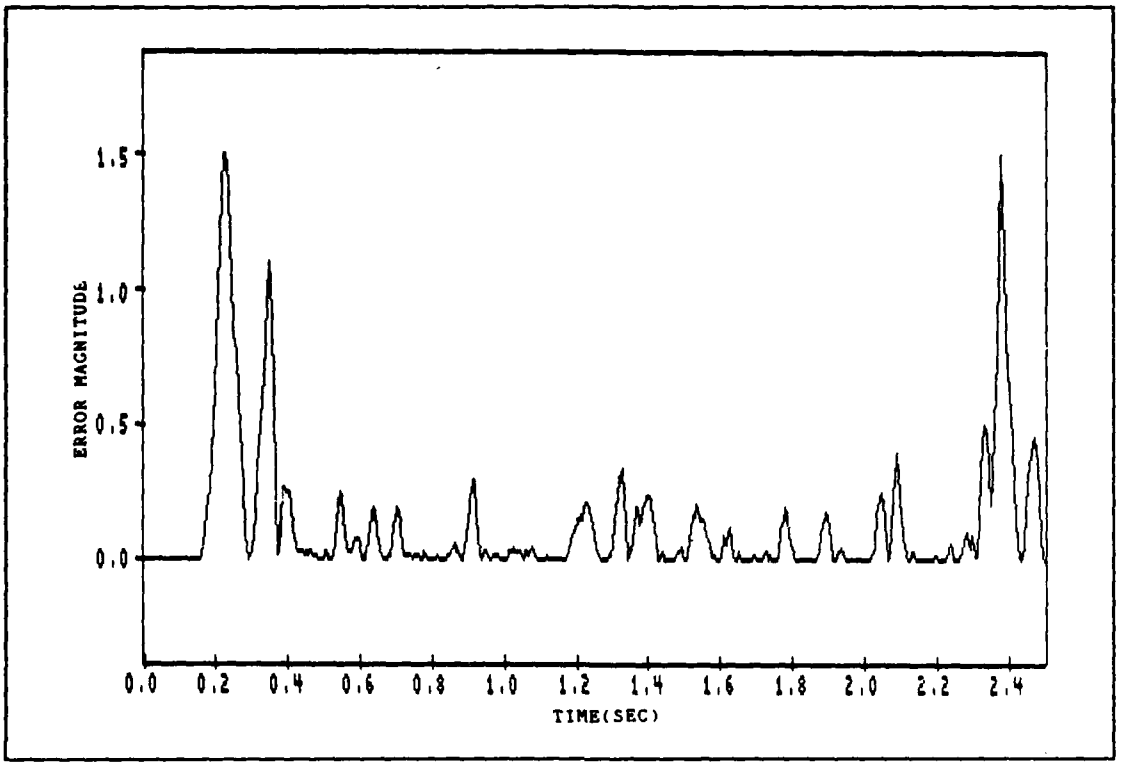

Figure 5.20. Experiment Five Error Magnitude

Adaptive Processing Using Human Signals

Based on the experimental filtering results and comparisons of the error signals, it was determined that actual ERF filtering would proceed using a filter size of 20 weights and a convergence factor of 0.005 and the methods used in Experiment Three would be repeated using actual human visual and audio data.

As in the previous experiments, five visual ERF signals were applied to the desired signal input with the simultaneously recorded ERP signals applied to the reference input. Based on the modeling experiments, no additional signal enhancement was gained by using more than five signals. As

shown in figure 5.21, a single filtered response (the third ERF of the five concatenated signals) taken from the filter output signal shows a typical ERF. Any judgement on the accuracy of this signal is impossible because a complete a priori knowledge of the ERF signal is not available. However, comparisons can be made to the ensemble average of 80 signals shown in figure 5.22. A close approximation is made to the general shape of the ensemble averaged signal as far as the location of signal peaks is concerned. However, a delay caused by filter processing and the low convergence factor is evident.

After reviewing the above filtering results, it was determined that an optimization of the convergence factor was necessary in order to reduce the filter output delay. Due to the non-stationary nature of the ERF and ERP signals, rapid convergence of the LMS filter (without sacrificing too much noise in the process) is required. Recall from Chapter II that the optimum weight vector, $\underline{W}^*$, is dependent upon the inverse of the filter input correlation matrix, $\underline{R}$, and the cross-correlation matrix between the desired input and the filter input, $\underline{P}$. Each of these matrices can vary from response to response resulting in a constant shifting of the performance surface. Therefore, a rapid convergence rate is required in order to track a moving performance surface where the lateral movement of the surface is primarily due to a change in the cross-correlation matrix, $\underline{P}$.

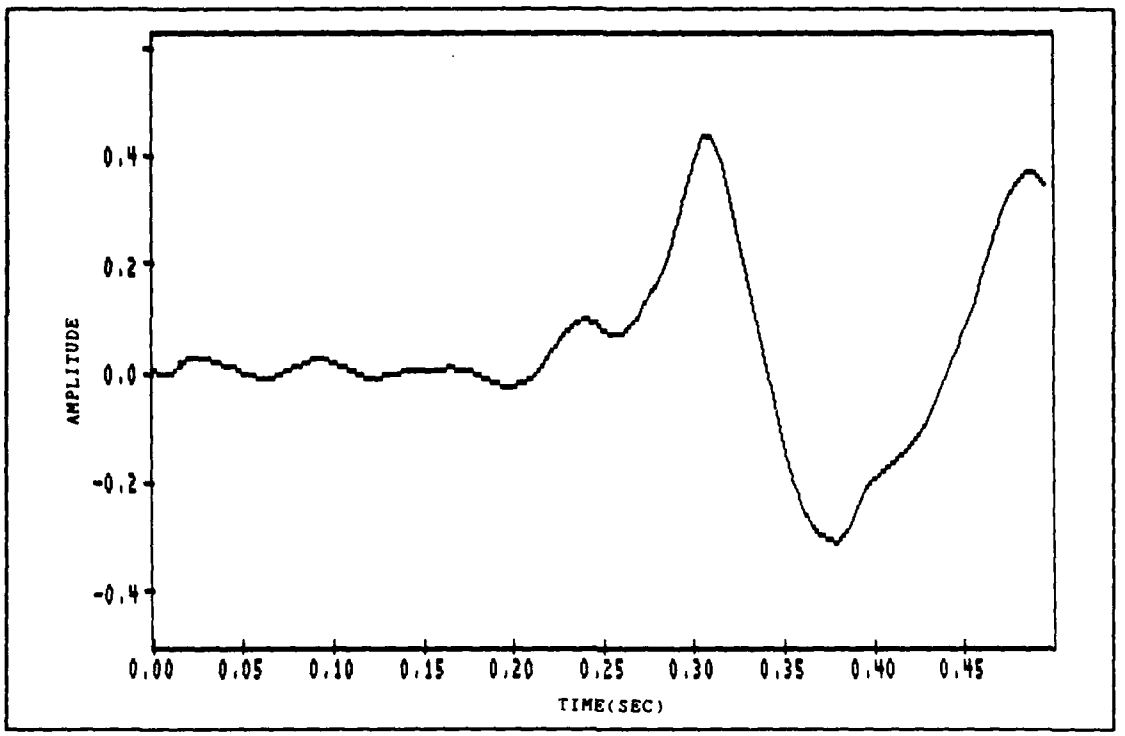

5.21. Single Response Filter Ouput

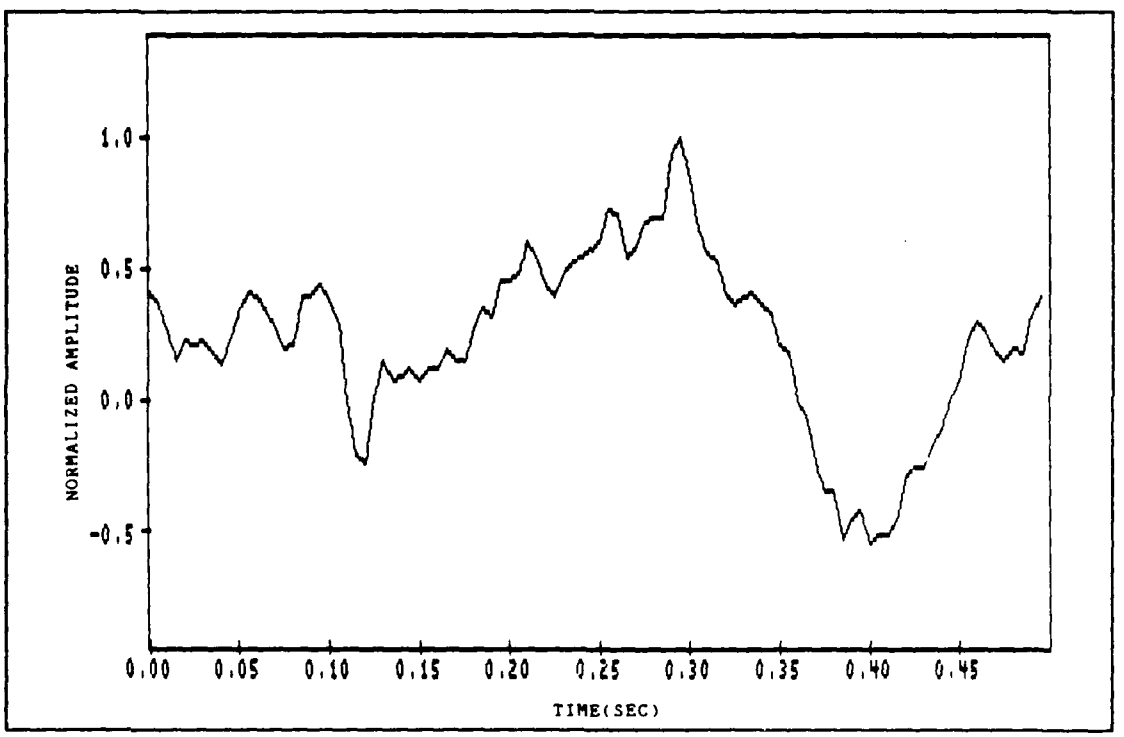

Figure 5.22. Average of 80 Responses

Optimization of the convergence factor was implemented by modifying the previous LMS program to vary μ based on the input signal power. From the previous discussion on choosing a value for μ, it was determined that its range is limited by the following:

$$0 < \mu < \frac{1}{n \cdot (\text{signal power})} \tag{5.2}$$

where n is the number of weights or filter size. This leads to a new definition of μ that varies depending on the signal input power. This is defined as follows:

$$\mu(k) = \frac{\alpha}{\beta + \underline{X}^T(k)\underline{X}(k)} \tag{5.3}$$

where α is the normalized adaptation constant and β is a constant used to keep $\mu(k)$ from becoming too large when the input signal power is very small. Using equation 5.3 in the LMS algorithm results in a constantly updated convergence factor where $\mu(k)$ is large when the input power is small and is small when the input power is large. The result is a filter that adapts more quickly without a large noise sacrifice. A listing of the Normalized LMS program is included in Appendix B. (10:83)

A plot of a single Normalized LMS output signal is shown in figure 5.23 (the third ERF signal out of five responses). Figure 5.24 is an overplot of this same

filtered signal with the unfiltered ERP desired input signal. A comparison of the Normalized LMS filter output with the previous LMS filter output in figure 5.21 shows that the lag due to filter processing is reduced.

To further evaluate the Normalized LMS filter performance, an audio ERF signal was applied to the desired input with its time sequenced ERP signal applied to the reference input. Figure 5.25 is the third response out of five output audio tone responses. Again, this signal is compared with an ensemble average of audio responses, shown in figure 5.26 with an overplot of the filtered signal of figure 5.25. In general, the waveform peaks are as evident in the single waveform as they are in the averaged signal (in this case the ensemble average included only 26 signals due to the limited availability of audio response data).

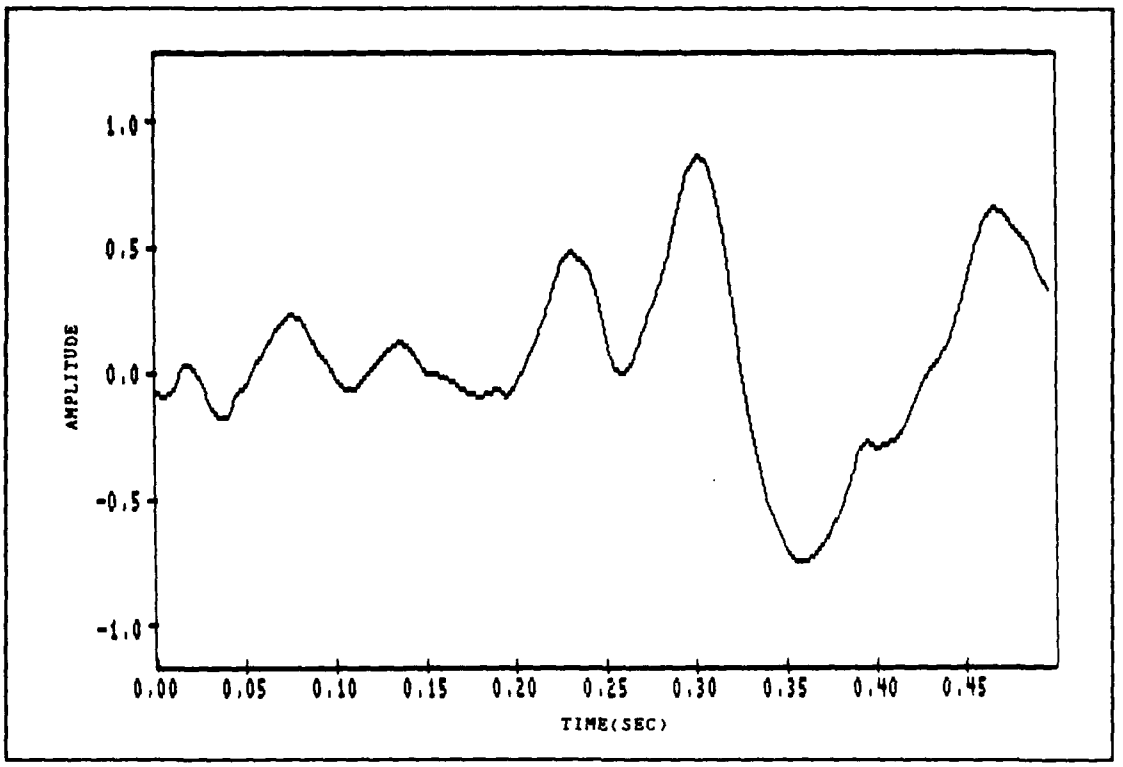

Figure 5.23. Normalized LMS Filter Output

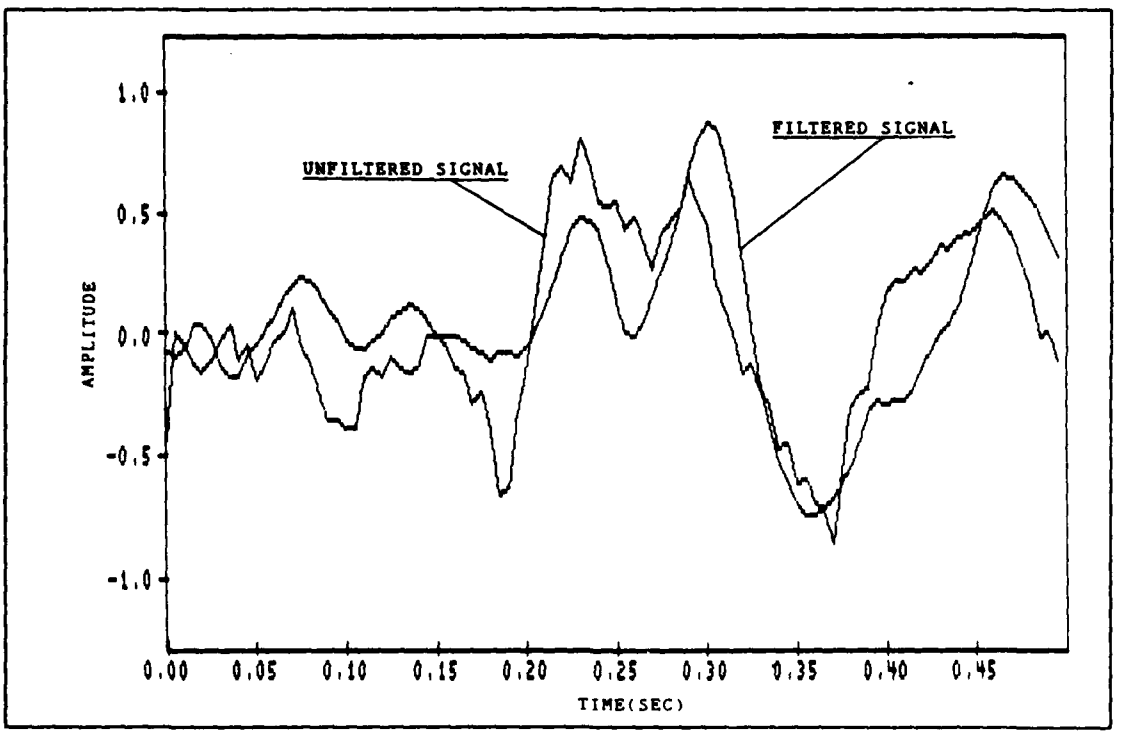

Figure 5.24. Filtered and Unfiltered Signals

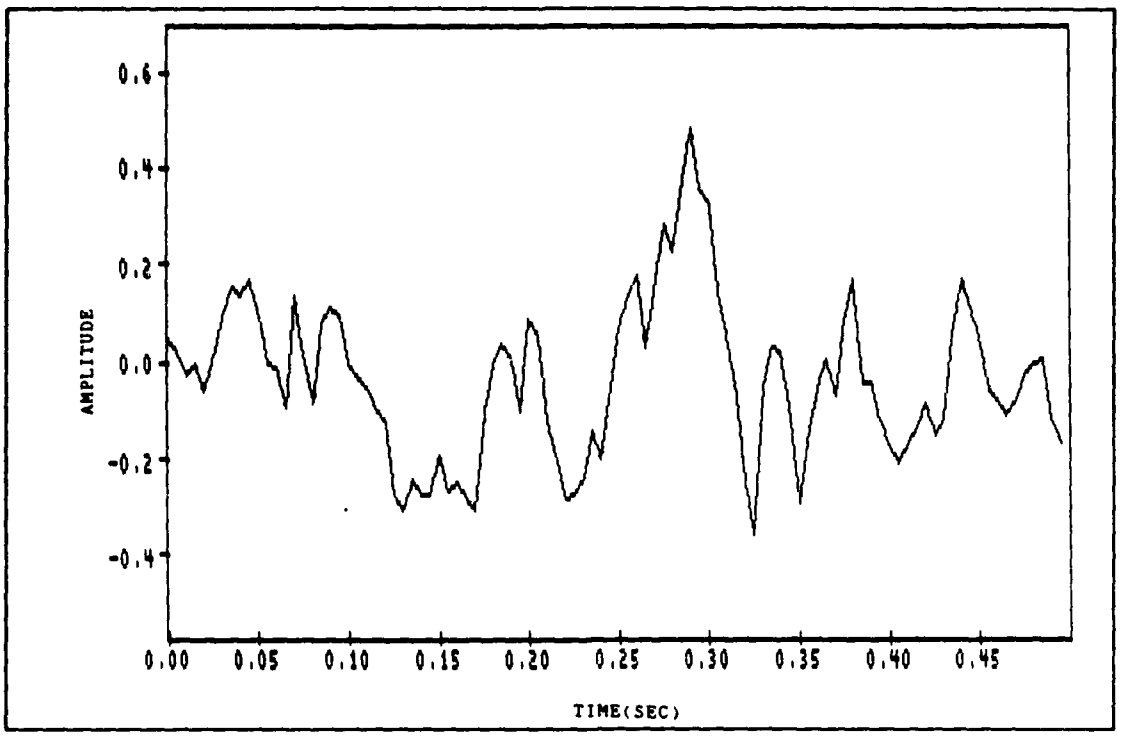

Figure 5.25. Filtered Audio Response

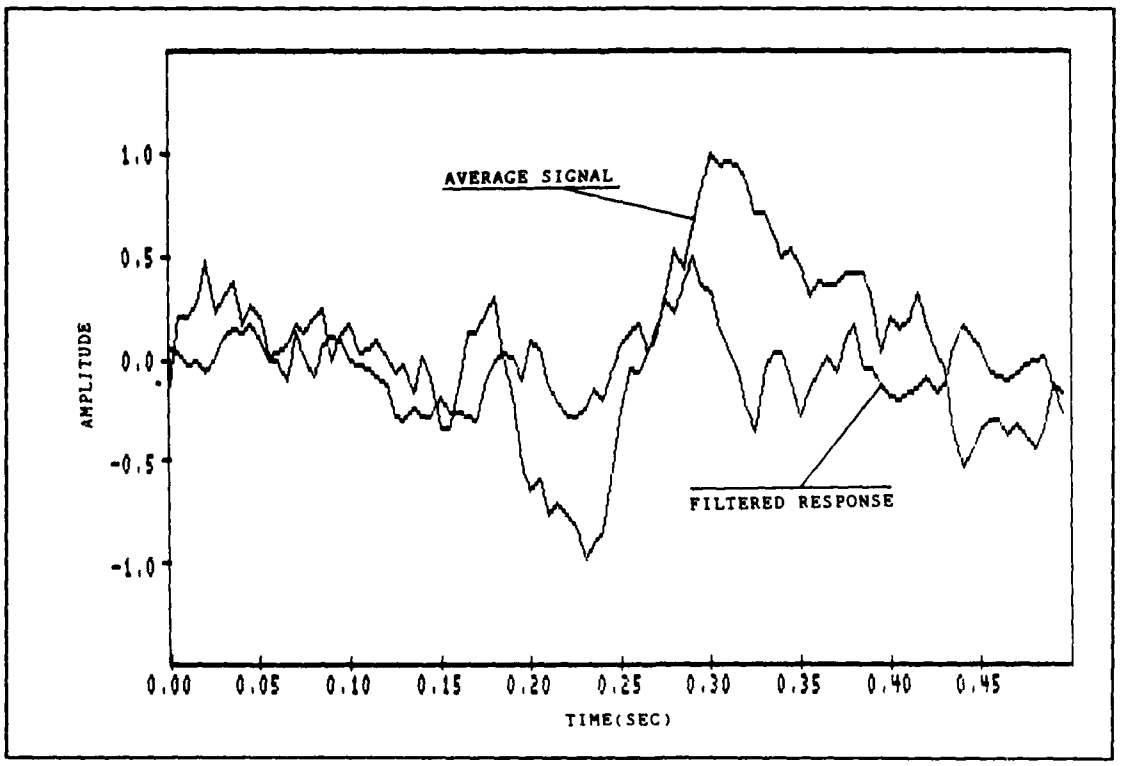

Figure 5.26. Filtered Audio Response and Average Signal

VI. Conclusions and Recommendations

Conclusions

This research investigated the feasibiltiy of using adaptive processing techniques, in the form of the Least-Mean-Squares (LMS) algorithm, to filter out unwanted MEG background noise from the evoked response field. It is hoped that the identification of these evoked fields, the brain's reaction to an audio or visual stimulus, will make it possible to localize specific origins and patterns of thought in the human brain. Several brain mapping experiments have been attempted with mixed success due to the difficulty in accurately identifying the evoked response field within a large background noise field. Typically, ensemble averaging of many signals is required in order to identify the basic shape of the response waveform. However, ensemble averaging requires that many signals be measured and recorded. Additionally, signal information such as time lags and true peak locations may be lost in the averaging process.

The ultimate goal of this research was to be able to filter a single evoked response field, using the evoked response potential as a reference signal, such that no signal averaging would be required to identify the location and amplitude of significant signal peaks. By modeling and adding noise to the signals of interest it was shown that a

significant amount of noise could be removed from the filtered signal. It was also shown that the higher the correlation between the desired signal and reference signal, the more effectively the desired signal will be enhanced. Time lags between the desired signal and the reference signal made it more difficult to identify signal peaks but identification was still possible in most cases.

Comparisons of single evoked response field signals with ensemble averages of real human signals showed a high correlation in most cases. This was especially true of the visual response signals. Although the signal peaks were visible on the audio response plots, they were more difficult to differentiate than the visual response filtered signals. This was most likely due to the higher noise content that the audio signals exhibited. Even so, it was still possible to filter five audio response signals and then use ensemble averaging to improve the signal-to-noise ratio. Comparisons of the five ensemble averaged signals with a much higher number of ensemble averaged signals that were not filtered showed similar waveform traits. An example of this comparison is shown in figures 6.1 and 6.2. In Experiment Five presented previously, five ERF signal models with added human MEG background signals were filtered using the original LMS adaptive algorithm. These same five signals were again filtered, this time using the normalized LMS, and ensemble averaged. Figure 6.1 is a plot of the

average of the five modeled signals. Figure 6.2 is a plot of 20 averaged signals with no filtering. Distinctive characteristics of the waveforms are difficult to pick out in both cases; however, the general shape of the waveform, including period and amplitude, is at least as good in the filtered plot as it is in the non-filtered plot. This leads to the conclusion that the current procedure of waveform averaging of up to 100 signals can be reduced by using adaptive processing techniques.

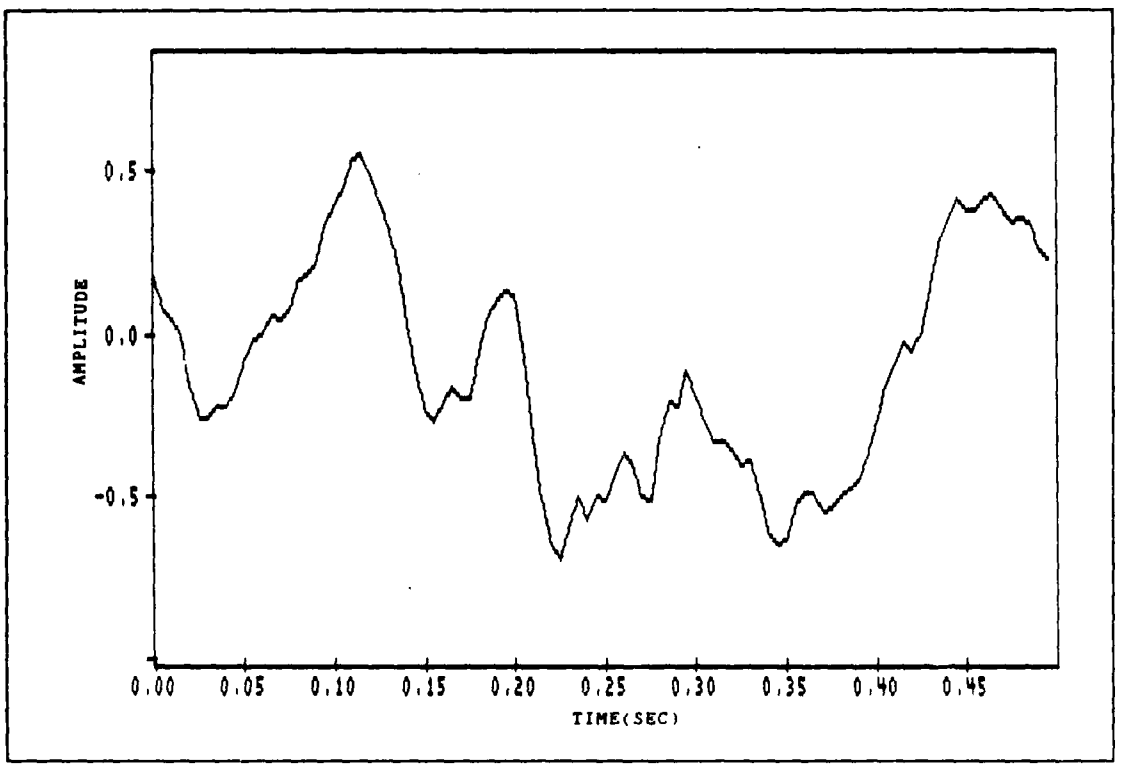

Figure 6.1. Average of Five Filtered Signals

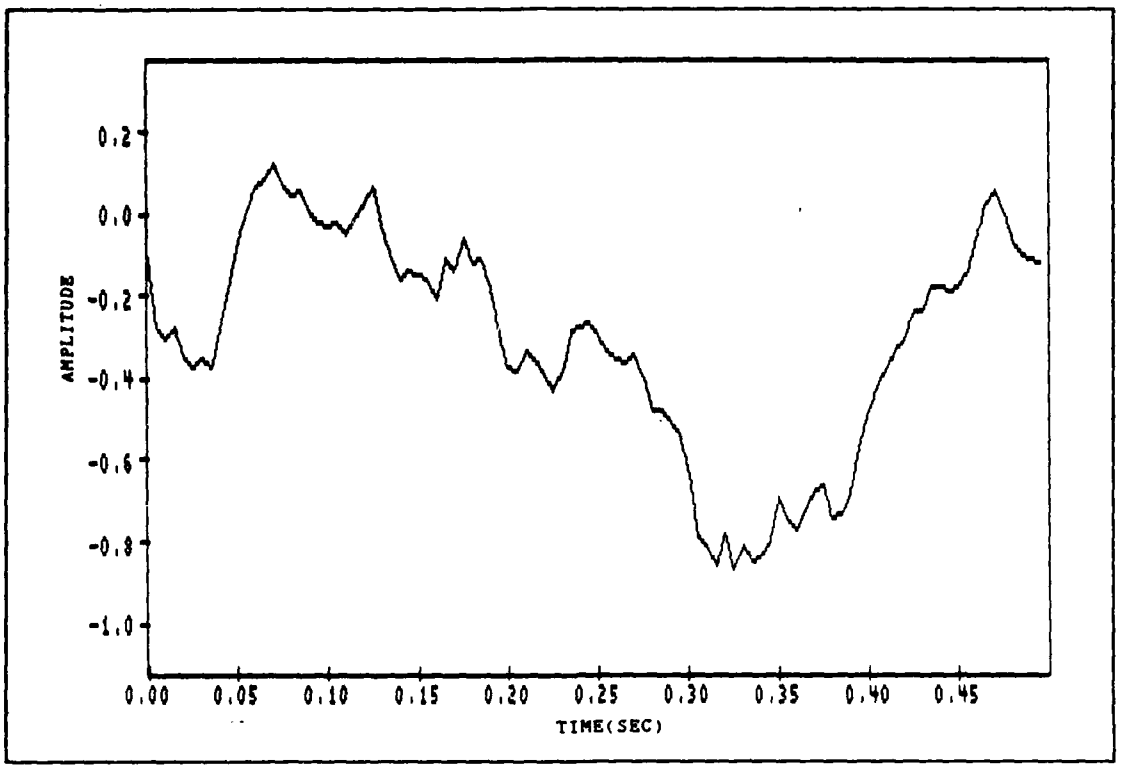

Figure 6.2. Average of 20 Unfiltered Signals

Recommendations

This research focused on the feasibility of using adaptive processing techniques to improve evoked response field signal-to-noise ratios. The basic LMS algorithm was used with a normalizing modification added to decrease the filter convergence time. Additional adaptive filtering techniques are available for further research on this subject.

Accelerated versions of the LMS algorithm can be found in Treichler, et al, along with the Recursive Least Square (RLS) algorithm (10:86-104). The major advantage of the RLS algorithm is that the optimum weight vector, $\underline{W}^*$, is computed

during each iterative step thus insuring that the overall optimum weight vector is found at the last input data point. A price is paid in programming complexity when implementing this algorithm.

Another possible adaptive filter implementation is the Griffith's Algorithm. Its primary advantage is that the desired input signal does not have to be known exactly; however, the correlation function between the desired signal and the filter input signal must be known. The expected value or average of the cross-correlation vector is substituted for the cross-correlation vector by itself. (10:85)

Future study of the brain's response to some outside stimulus and its relationship to magnetic fields requires that background MEG noise be minimized. Any of the above mentioned adaptive algorithms could be used as a basis for further research on this subject.

Appendix A: The LMS Program

```
{$R+}

PROGRAM LMS1;

{ Program Name:  LMS1 }
{ Programming Language:  Pascal V.4 }
{ Program Writer:  Roger A. Wood}
{ This program is designed to adaptively filter a given
  input signal "S" based on a reference signal "N". It is
capable of filtering up to 8000 data points using up to
  50 filter weights. }


USES
   CRT, PRINTER;

CONST
   DataSizeMax = 7999; {8000 data points @ 200 samples/sec.}

TYPE
   DataArray = ARRAY[0..DataSizeMax] OF REAL;
   Data = ^DataArray;
   FileNumber = STRING[3];

VAR
   WeightNumber, Clock, FilterSize  :INTEGER;
   PointerStart  :^REAL;
   u, Error, Out_Y, Signal  :REAL;
   N, S, E, Y :TEXT;
   In_X  :DATA;
   Weight  :ARRAY[0..50] OF REAL;
   DataRunNumber  :FileNumber;
   EDATFILE, MDATFILE  :STRING[20];
   CHECKBREAK  :BOOLEAN;

PROCEDURE Clear_Space;
{This procedure clears the screen.}

BEGIN
   GOTOXY(1,22); CLREOL;
   GOTOXY(1,23); CLREOL;
   GOTOXY(1,24); CLREOL;
END;
```

```
PROCEDURE Get_Filter_Constants;
{This procedure initializes the filter constants and reads
in the value of u (the constant convergence constant).}

BEGIN
   CLRSCR;
   GOTOXY(1,22);
   WRITE('Enter data run number (use a number between 000
and 999).   >');
   READ(DataRunNumber);
   CLRSCR;
   GOTOXY(1,22);
   WRITE('Enter number of weights in filter (2 to 50).  >');
   READ(FilterSize);
   FilterSize:=(FilterSize-1);
   CLRSCR;
   GOTOXY(1,22);
   WRITE('Enter value of "u" (0.0 to 1.0)  >');
   READ(u);
END;


PROCEDURE Initialize_Data_Arrays;
{This procedure initializes the filter weights to zero.}

BEGIN
   FOR WeightNumber:=0 TO FilterSize DO
   BEGIN
      Weight[WeightNumber]:=0;   {Set all weights to zero
initially.}
   END;
END;

PROCEDURE  Run_Filter;
{********* THE ADAPTIVE FILTER ********************}

BEGIN
   CLEAR_SPACE;

   {Read in the MEG data}
   ASSIGN(S,'A:MEG.DAT');
   RESET(S);
   GOTOXY (1,22);

   {Read in the EEG data}
   ASSIGN(N,'A:EEG.DAT');
   RESET(N);
   MARK(PointerStart);
```

```
    NEW(IN_X);

    {Set up the output files}
    ASSIGN(E,CONCAT('A:E',DataRunNumber,'.DAT'));
    REWRITE(E);
    ASSIGN(Y,CONCAT('A:Y',DataRunNumber,'.DAT'));
    REWRITE(Y);
    GOTOXY(5,24); WRITELN('Running adaptive filter.');
    Clock:=0;

    {Start running the filter}
    WHILE NOT EOF(S) DO
    BEGIN
       READ(S,Signal);
       READ(N,IN_X^[Clock]);  write('clock = ', clock);
       OUT_Y:=0;
       IF Clock=0 THEN
       BEGIN
          Error:=Signal;
          WRITELN(E,Error);
          WRITELN(Y,OUT_Y);
          WRITELN(error:9:4,OUT_Y:9:4);
          Clock:=Clock+1;
       END ELSE
       BEGIN
          IF (Clock-FilterSize)<=0 THEN
          BEGIN
FOR WeightNumber:=0 TO Clock-1 DO
             BEGIN
                Weight[WeightNumber]:=Weight[WeightNumber]+
                2*u*Error*IN_X^[(Clock-1-WeightNumber)];
                OUT_Y:=OUT_Y+Weight[WeightNumber]*
                IN_X^[Clock-WeightNumber];
             END;
             Error:=Signal-OUT_Y;
             WRITELN(E,Error);
             WRITELN(Y,OUT_Y);
             WRITELN(error:9:4,OUT_Y:9:4);
             Clock:=Clock+1;
          END ELSE
          BEGIN
             FOR WeightNumber:=0 TO FilterSize DO
             BEGIN
                Weight[WeightNumber]:=Weight[WeightNumber]+
                2*u*Error*IN_X^[(Clock-1-WeightNumber)];
                OUT_Y:=OUT_Y+Weight[WeightNumber]*
                IN_X^[Clock-WeightNumber];
             END;
             Error:=Signal-OUT_Y;
             WRITELN(E,Error);
             WRITELN(Y,OUT_Y);
             WRITELN(error:9:4,OUT_Y:9:4);
```

```
            Clock:=Clock+1;
          END;
       END;
    END;
    RELEASE(PointerStart);
    CLOSE(S);
    CLOSE(N);
    CLOSE(E);
    CLOSE(Y);
END;


{******************** MAIN PROGRAM ********************}

BEGIN

Get_Filter_Constants;
Initialize_Data_Arrays;
Run_Filter;
END.
```

Appendix B: Modified LMS Program

```
{$R+}

PROGRAM LMS2;

{ Program Name: LMS2 }
{ Programming Language:  PASCAL V.4 }
{ Program Writer:  Roger A. Wood}
{ This program is a modification of LMS1.  The convergence
factor u(clock) in this case change constantly depending on
the power of the input signal.  The input data is limited to
2000 data points in this program. }


USES
   CRT, PRINTER;

CONST
   DataSizeMax = 1999; {2000 data points @ 200 samples/sec.}

TYPE
   DataArray = ARRAY[0..DataSizeMax] OF REAL;
   Data = ^DataArray;
   FileNumber = STRING[3];

VAR
   WeightNumber, Clock, FilterSize, I  :INTEGER;
   PointerStart  :^REAL;
   Error, Out_Y, Signal, A, B  :REAL;
   N, S, E, Y :TEXT;
   In_X  :DATA;
   u,pwr :DataArray;
   Weight  :ARRAY[0..80] OF REAL;
   DataRunNumber  :FileNumber;
   EDATFILE, MDATFILE  :STRING[20];
   CHECKBREAK  :BOOLEAN;

PROCEDURE Clear_Space;
{This procedure clears the screen.}

BEGIN
   GOTOXY(1,22); CLREOL;
   GOTOXY(1,23); CLREOL;
   GOTOXY(1,24); CLREOL;
END;
```

```
PROCEDURE Get_Filter_Constants;
{This procedure initializes the filter constants and reads
in the value of u (the constant convergence constant).}

BEGIN
   CLRSCR;
   GOTOXY(1,22);
   WRITE('Enter data run number (use a number between 000
and 999).   >');
   READ(DataRunNumber);
   CLRSCR;
   GOTOXY(1,22);
   WRITE('Enter number of weights in filter (2 to 80).  >');
   READ(FilterSize);
   FilterSize:=(FilterSize-1);
   CLRSCR;
   GOTOXY(1,22);
   WRITE('Enter value of "A" (0.0 to 2.0)  >');
   READ(A);
END;


PROCEDURE Initialize_Data_Arrays;
{This procedure initializes the filter weights to zero.
Also, the power and convergence factor, u, arrarys are
 also initialized.}

BEGIN
   FOR WeightNumber:=0 TO FilterSize DO
   BEGIN
      Weight[WeightNumber]:=0;   {Set all weights to zero
initially.}
   END;
   FOR I:= 0 TO DATASIZEMAX DO
   BEGIN
     PWR(I):= 0;
     U(I):= 0;
   END;
END;

PROCEDURE  Calc_x_power;

VAR
   I :integer;
   BEGIN
   If (Clock-Filtersize+1) >= 0 Then
   BEGIN
      FOR I := CLOCK DOWNTO (CLOCK - FILTERSIZE + 1) DO
      PWR[CLOCK] := PWR[CLOCK] + IN_X^[I]*IN_X^[I];
      END ELSE
      BEGIN
         FOR I:=0 TO CLOCK DO
```

```
            PWR[CLOCK] :=PWR[CLOCK] + IN_X^[I]*IN_X^[I];
            END;
         END;



   PROCEDURE  Run_Filter;
{************* THE ADAPTIVE FILTER *********************}

BEGIN
   CLEAR_SPACE;

   {Read in the MEG data}
   ASSIGN(S,'A:MEG.DAT');
   RESET(S);
   GOTOXY (1,22);

   {Read in the EEG data}
   ASSIGN(N,'A:EEG.DAT');
   RESET(N);
   MARK(PointerStart);
   NEW(IN_X);

   {Set up the output files}
   ASSIGN(E,CONCAT('A:E',DataRunNumber,'.DAT'));
   REWRITE(E);
   ASSIGN(Y,CONCAT('A:Y',DataRunNumber,'.DAT'));
   REWRITE(Y);
   GOTOXY(5,24); WRITELN('Running adaptive filter.');
   Clock:=0;

   {Start running the filter}
   WHILE NOT EOF(S) DO
   BEGIN
      READ(S,Signal);
      READ(N,IN_X^[Clock]);  write('clock = ', clock);
      OUT_Y:=0;
      CALC_X_POWER;
      U[CLOCK]:= A/(0.1+PWR[CLOCK]);
      IF Clock=0 THEN
      BEGIN
         Error:=Signal;
         WRITELN(E,Error);
         WRITELN(Y,OUT_Y);
         WRITELN(error:9:4,OUT_Y:9:4);
         Clock:=Clock+1;
      END ELSE
      BEGIN
         IF (Clock-FilterSize)<=0 THEN
         BEGIN
```

```
FOR WeightNumber:=0 TO Clock-1 DO
            BEGIN
             Weight[WeightNumber]:=Weight[WeightNumber]+
             2*u[clock]*Error*IN_X^[(Clock-1-WeightNumber)];
               OUT_Y:=OUT_Y+Weight[WeightNumber]*
               IN_X^[Clock-WeightNumber];
            END;
            Error:=Signal-OUT_Y;
            WRITELN(E,Error);
            WRITELN(Y,OUT_Y);
            WRITELN(error:9:4,OUT_Y:9:4);
            Clock:=Clock+1;
         END ELSE
         BEGIN
            FOR WeightNumber:=0 TO FilterSize DO
            BEGIN
             Weight[WeightNumber]:=Weight[WeightNumber]+
             2*u[clock]*Error*IN_X^[(Clock-1-WeightNumber)];
               OUT_Y:=OUT_Y+Weight[WeightNumber]*
               IN_X^[Clock-WeightNumber];
            END;
            Error:=Signal-OUT_Y;
            WRITELN(E,Error);
            WRITELN(Y,OUT_Y);
            WRITELN(error:9:4,OUT_Y:9:4);
            Clock:=Clock+1;
          END;
      END;
   END;
   RELEASE(PointerStart);
   CLOSE(S);
   CLOSE(N);
   CLOSE(E);
   CLOSE(Y);
END;


{******************* MAIN PROGRAM ******************}

BEGIN

Get_Filter_Constants;
Initialize_Data_Arrays;
Run_Filter;
END.
```

Bibliography

1. Carelli, P. "Magnetoencephalography," Proceedings of a NATO Advanced Study, Institute On Biomagnetism 469-482. Grottaferrata (Rome), Italy: Plenum Press, New York, 1983.

2. Cohen, David. "Introduction," Proceedings of a NATO Advanced Study, Institute on Biomagnetism 5-16. Grottaferrata (Rome), Italy: Plenum Press, New York, 1983.

3. De Rego, Paul J. "Test and Evaluate Contemporary Algorithms Designed for the Detection and Estimation of Single Evoked Neural Responses," Proposed AFIT Thesis Topic. Air Force Armstrong Aerospace Medical Research Laboratory, Human Engineering Division, (AFSC), Wright Patterson AFB OH, No Date.

4. -----. A Multipole Model of the Observed Cerebral Cortex Magnetic Field. MS Thesis AFIT/GE/ENG/84D-23. School of Engineering, Air Force Institute of Technology (AU), Wright-Patterson AFB OH, December 1984.

5. Dowler, Michael G. Retinoptic Mapping of the Human Visual System With Magnetoencephalography. MS Thesis AFIT/GEP/ENP/87D-6. School of Engineering, Air Force Institute of Technology (AU), Wright-Patterson AFB OH, December 1987.

6. Gevins, Alan S. "Analysis of the Electromagnetic Signals of the Human Brain: Milestones, Obstacles, and Goals," IEEE Transactions on Biomedical Engineering, 34: 833-847 (December 1984).

7. Hari, R. et al. "Biomagnetism in the Study of Brain Function," Proceedings of the Fifth World Conference on Biomagnetism. 221-234. Vancouver: Pergamon Press, 1985.

8. McGillem, C. D. et al. Detection, Estimation, and Multidimensional Processing of Single Evoked Potentials. EEG Signal Processing Laboratory, School of Electrical Engineering, Purdue University, West Lafeyette, Indiana, August 1985.

9. Thakor, Nitish V. "Adaptive Filtering of Evoked Potentials," IEEE Transactions On Biomedical Engineering, 34: 6-13 (January 1987).

10. Treichler, John R. et al. Theory and Design of Adaptive Filters. New York: John Wiley and Sons, 1987.

11. Widrow, Bernard. Adaptive Signal Processing. Englewood Cliffs, N.J.: Prentice Hall Inc., 1985.

12. Widrow, Bernard et al. "Stationary and Nonstationary Learning Characteristics of the LMS Adaptive Filter," Proceedings of the IEEE, 34: 1153-1162 (August 1976).

13. ----. "On the Statistical Efficiency of the LMS Algorithm with Nonstationary Inputs," IEEE Transactions on Information Theory, 30: 211-221 (March 1984).

14. Williams, Capt. Robert. Instructor. Personal Interviews. School of Engineering, Air Force Institute of Technology (AU), Wright-Patterson AFB, OH, 1 December 1987 through 8 February 1988.

15. Yama, K. et al. "EOG Canceling in EEG: An Adaptive Process," Proceedings of the Ninth Annual Conference of the Engineering in Medicine and Biology Society. 860-868. Boston: The Institute of Electrical and Electronics Engineers, Inc., 1987.

16. Yu, K. B. et al. "Optimum Filter for Estimating Evoked Potential Waveforms," IEEE Transactions on Biomedical Engineering, 30: 730-736 (November 1983).

VITA

Captain Wood was born [redacted] graduated from high school in [redacted] He then enlisted in the United States Army where he worked as a Cryptological Equipment Repairmen at assignments in Seoul, Korea and Fort Huachuca, Arizona. Following his separation from the Army in 1980, Captain Wood attended the Ohio State University in Columbus, Ohio where he majored in Electrical Engineering. He also served as a Cryptological Equipment Repairmen in the Ohio Air National Guard while attending Ohio State. During his senior year, he participated in the Air Force's College Senior Engineering Program. After receiving his Bachelor of Science degree in Electrical Engineering in March 1984, he attended Officer Training School at Lackland AFB, Texas. Following his commissioning in June 1984, he was assigned to the Fleet Satellite Communications program office at Space Division, Los Angeles AFS, California where he worked as a satellite subsystem engineer responsible for the electrical powere subsystem and telemetry, tracking, and control subsystem. In May 1987, Captain Wood was reassigned to the School of Engineering, Air Force Institute of Technology.

UNCLASSIFIED
SECURITY CLASSIFICATION OF THIS PAGE

REPORT DOCUMENTATION PAGE

Form Approved
OMB No. 0704-0188

1a. REPORT SECURITY CLASSIFICATION UNCLASSIFIED	1b. RESTRICTIVE MARKINGS
2a. SECURITY CLASSIFICATION AUTHORITY	3. DISTRIBUTION/AVAILABILITY OF REPORT Approved for public release; distribution unlimited.
2b. DECLASSIFICATION/DOWNGRADING SCHEDULE	
4. PERFORMING ORGANIZATION REPORT NUMBER(S) AFIT/GE/ENG/88D-62	5. MONITORING ORGANIZATION REPORT NUMBER(S)
6a. NAME OF PERFORMING ORGANIZATION School of Engineering 6b. OFFICE SYMBOL (If applicable) AFIT/ENG	7a. NAME OF MONITORING ORGANIZATION
6c. ADDRESS (City, State, and ZIP Code) Air Force Institute of Technology Wright-Patterson AFB OH 45433-6583	7b. ADDRESS (City, State, and ZIP Code)
8a. NAME OF FUNDING/SPONSORING ORGANIZATION 8b. OFFICE SYMBOL (If applicable)	9. PROCUREMENT INSTRUMENT IDENTIFICATION NUMBER
8c. ADDRESS (City, State, and ZIP Code)	10. SOURCE OF FUNDING NUMBERS PROGRAM ELEMENT NO. / PROJECT NO. / TASK NO. / WORK UNIT ACCESSION NO.
11. TITLE (Include Security Classification) See Box 19	
12. PERSONAL AUTHOR(S) Roger A. Wood, B.S., Capt, USAF	
13a. TYPE OF REPORT MS Thesis 13b. TIME COVERED FROM _____ TO _____ 14. DATE OF REPORT (Year, Month, Day) 1988 December 15. PAGE COUNT 93	
16. SUPPLEMENTARY NOTATION	

17. COSATI CODES			18. SUBJECT TERMS (Continue on reverse if necessary and identify by block number)
FIELD	GROUP	SUB-GROUP	Magneto-encephalogram, Evoked Response Field Adaptive Signal Processing, Adaptive Filter
06	04		
23	01		

19. ABSTRACT (Continue on reverse if necessary and identify by block number)

Title: Electro-encephalogram Based Adaptive Estimation of Magneto-encephalogram Signals

Thesis Chairman: Robert Williams, Captain, USAF
Instructor, Electral Engineering

12 Jan 1989

20. DISTRIBUTION/AVAILABILITY OF ABSTRACT ☒ UNCLASSIFIED/UNLIMITED ☐ SAME AS RPT. ☐ DTIC USERS	21. ABSTRACT SECURITY CLASSIFICATION UNCLASSIFIED
22a. NAME OF RESPONSIBLE INDIVIDUAL Robert Williams, Captain, USAF	22b. TELEPHONE (Include Area Code) (513) 255-3708 22c. OFFICE SYMBOL AFIT/ENG

DD Form 1473, JUN 86 — Previous editions are obsolete. — SECURITY CLASSIFICATION OF THIS PAGE
UNCLASSIFIED

Adaptive signal processing techniques were used to filter out unwanted background noise from the evoked response field signals obtained from magneto-encephalogram measurements. A model of the evoked response field signals was first developed to test the adaptive algorithm in an environment corrupted by white gaussian noise. Several modeling experiments verified the feasibility of adaptive filtering using an enhancement design with a correlated signal representing the evoked potential response obtained from electro-enchephalogram measurements. The experimental results showed that signal estimation is improved by a strong correlation between the evoked response field and evoked response potential.

Following the modeling experiments, filtering of actual evoked responses was attempted. To obtain the evoked field data, an audio or visual stimulus was provided to a test subject located inside a shielded chamber. Time sequenced electro-encephalogram and magneto-encephalogram signals were recorded for later processing using an adaptive filter based on the least-mean-square algorithm. Accuracy of the filtered human data could not be quantified due to a lack of a priori knowledge of the exact signals before filtering. Comparisons of filtered responses with ensemble averaged responses of up to 80 signals showed waveform similarities.